Monatshefte für Chemie - Chemical Monthly (2022) 153:659–686
https://doi.org/10.1007/s00706-022-02938-4

REVIEW

Liquid chromatography and capillary electrophoresis in glycomic and glycoproteomic analysis

Katarina Molnarova[1] · Katerina Cokrtova[1] · Alice Tomnikova[1] · Tomas Krizek[1] · Petr Kozlik[1]

Received: 29 March 2022 / Accepted: 29 May 2022 / Published online: 21 June 2022

Abstract

Glycosylation is one of the most significant and abundant post-translational modifications in cells. Glycomic and glycoproteomic analyses involve the characterization of oligosaccharides (glycans) conjugated to proteins. Glycomic and glycoproteomic analysis is highly challenging because of the large diversity of structures, low abundance, site-specific heterogeneity, and poor ionization efficiency of glycans and glycopeptides in mass spectrometry (MS). MS is a key tool for characterization of glycans and glycopeptides. However, MS alone does not always provide full structural and quantitative information for many reasons, and thus MS is combined with some separation technique. This review focuses on the role of separation techniques used in glycomic and glycoproteomic analyses, liquid chromatography and capillary electrophoresis. The most important separation conditions and results are presented and discussed.

Graphical abstract

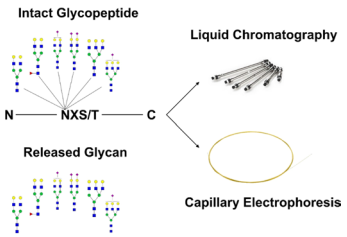

Keywords Capillary zone electrophoresis · Glycan separation · Glycopeptide separation · High-pressure liquid chromatography · Proteomics

Introduction

Glycomics and glycoproteomics are branches of proteomics that study, analyze, and characterize glycosylated proteins, i.e., proteins containing carbohydrates as post-translation modification [1]. Glycosylation is one of the most prominent and important post-translation modification of proteins [2], which plays a key role in many biological processes including molecular trafficking and clearance, cell–cell interaction, or antigen recognition [3]. Protein glycosylation includes a series of enzymatic reactions, which result in a formation of amino acid-glycan linkage. There are two major types of glycosylation, namely *N*- and *O*-glycosylation. In case of *N*-glycosylation, glycans are attached to the peptide via amide nitrogens of asparagine side chains, whereas *O*-glycosylation involves the attachment through the hydroxyl oxygen atom of serine or threonine side chain [4]. Furthermore, for the *N*-linked glycans, there is a known glycosylation sequin which begins with asparagine followed by any amino acid except proline and ends with either serine or threonine [5]. The most common monosaccharides attached to the peptide backbone include *N*-acetylglucosamine, *N*-acetylgalactosamine, glucose, galactose, fucose, mannose, and sialic acid [1]. In the last decade, glycopeptides have been used as diseases biomarkers ranging from various

✉ Petr Kozlik
petr.kozlik@natur.cuni.cz

[1] Department of Analytical Chemistry, Faculty of Science, Charles University, Prague, Czech Republic

types of cancer (ovarian [6], breast [7], prostate [8], hepatocellular carcinoma [9]) to congenital disorders [10] and Alzheimer's disease [11]. Moreover, glycopeptides are often used as biopharmaceuticals due to their favorable properties, such as good biological activity, increased bioavailability and improved serum half-life [12]. Among others, trastuzumab [13], vancomycin [14], or erythropoietin [15] are the most known drugs based on glycopeptides. To ensure the quality and safety of drug manufacturing, and to improve the development of potential biomarkers, the analysis of glycosylation is a crucial step. However, it is a highly challenging task as it requires the identification of both, glycosylation sites and glycan structures, simultaneously [16]. Mass spectrometry (MS) is a key technique in glycoproteomics. Unfortunately, MS alone does not always provide full structural and quantitative information for many reasons, (e.g., limited fragmentation, low ionization efficiency of glycopeptides in complex mixtures) and thus MS is combined with some separation technique, mainly with liquid chromatography (LC) or capillary zone electrophoresis (CZE). Although there are many reviews on the glycoproteomics [16–20], most of them focus on advances in MS-based glycoproteomics and only a minority on separation techniques.

In this review, we provide an overview of separation techniques (LC and CZE) used in analysis of glycopeptides and glycans. First, LC techniques in glycopeptides and glycans separations are introduced, including reversed-phase chromatography (RP-LC), hydrophilic interaction liquid chromatography (HILIC), chromatography on porous graphitized carbon (PGC) material, and multi-dimensional chromatography. Then we focus on the CZE used in glycopeptides and glycans separations.

Liquid chromatography in glycopeptide separation

Liquid chromatography is the most widely used technique for the separation of glycopeptides. In bottom-up, also known as shotgun proteomics, the glycopeptides are produced by enzymatic digestion of glycoproteins (usually by trypsin). The resulting glycopeptides are subsequently separated by either RP-LC, HILIC, or PGC. In the following chapters, we show the applications of these chromatographic modes in the separation of intact glycopeptides and released glycans. In addition to that, we show the potential of these techniques for the separation of glycopeptide isomers that differ in branching and/or linkage positions of the attached glycans.

The most studied glycopeptide isomers include those with core and outer arm fucosylation, and glycopeptides with sialic acid [21–25]. Moreover, in this chapter, we discuss the possibility of combining two different liquid chromatography techniques, namely RP-HILIC, RP-PGC, and HILIC-PGC. These separation methods often use tandem mass spectrometry (MS/MS) detection [26–29] but some of them utilize UV detection [30–34]. In Table 1, we summarize the most important characteristics of the methods and approaches that we discuss in detail in the following chapters.

Reversed phase chromatography

Even though chromatography on RP stationary phases is one of the most widely used separation methods utilized in glycoproteomics, most of the researchers use it as a mere preliminary step before their characterization by MS and do not focus on the separation itself [35–41]. The most frequently used RP-LC columns in glycoproteomics separations are packed with octadecyl (C18) bounded silica gel. In RP-LC, the separation of glycopeptides is mainly based on hydrophobicity of the peptide backbone with additional influence of the glycan moiety [42–46]. Despite the fact that RP-LC is the most utilized separation technique, it is not able to adequately resolve different glycoforms attached to the same peptide backbone [43, 47, 48]. Molnarova et al. [43] separated the glycopeptides of human immunoglobulin G (IgG) on a C18 BEH (ethylene bridged hybrid) column (2.1 × 100 mm; 1.7 µm). The separation is shown in Fig. 1. The peptide backbone of the studied glycopeptides only differs in two amino acids (IgG1: EEQYNSTYR, IgG2: EEQENSTFR). Because phenylalanine is more hydrophobic than tyrosine, IgG2 glycopeptides eluted after the IgG1 glycopeptides.

The research group of Hernandez-Hernandez [49] employed Hypersil HyPurity C18 column (100 mm × 2.1 mm; 3.0 µm) for the separation of *O*-glycopeptides of bovine caseinomacropeptide. In this study, they compare the retention of both glycosylated and non-glycosylated peptides. In case of glycosylated peptides, the retention was lower and peaks were less resolved than in case of non-glycosylated forms. Hong's research team [50] used an Agilent Eclipse plus C18 column (2.1 × 100 mm; 1.8 µm) for the separation of IgG glycopeptides from glycopeptide standard and human serum. They observed that the non-glycosylated peptides of IgG eluted after the glycopeptides. The earlier elution of glycopeptides was favorable in terms of their electrospray ionization, which might be suppressed by the simultaneous ionization of non-glycosylated peptides.

Although the presence of glycans has only a secondary effect on the retention of glycopeptides, there are studies that investigated the influence of different glycan units on retention in RP-LC [42, 46, 51, 52]. The Ozohanics research group [53] observed that on a C18 column (0.075 × 200 mm; 1.7 µm) neutral glycans

Table 1 An overview of glycopeptide separation by different liquid chromatography approach. Columns, column dimensions, column manufacturers, analytes, mobile phase compositions and references are summarized

	Column, column dimensions and manufacturer	Analyte	Mobile phase composition	References
Reversed phase chromatography	Acquity UPLC BEH C18 2.1 × 100 mm; 1.7 µm; Waters Corporation	IgG standard from human plasma	ACN with 0.1% FA/ 0.1% FA	[43]
	Hypersil HyPurity C18 2.1 × 100 mm; 3.0 µm; Thermo Fisher Scientific	*O*-glycopeptides of bovine caseinomacropeptide	ACN with 0.1% FA/ 0.1% FA	[49]
	Agilent Eclipse plus C18 2.1 × 100 mm; 1.8 µm; Agilent Technologies	IgG standard from human plasma	90% ACN with 0.1% FA/ 3% ACN with 0.1% FA	[50]
	NanoAcquity UPLC BEH C18 0.075 × 200 mm; 1.7 µm; Waters Corporation	Human A1GP Haptoglobin	ACN with 0.1% FA/ 0.1% FA	[53]
	Acclaim PepMap™ 100 C18 0.075 × 150 mm; Thermo Fisher Scientific	ABCA4 (integral membrane protein)	ACN/water	[52]
	Acclaim PepMap™ 100 C18 0.075 × 150 mm; 2.0 µm; Thermo Fisher Scientific	Bovine fetuin, human A1GP, human erythropoietin (derivatized sialic acids)	ACN with 0.1% FA/ 0.1% FA	[56]
	Acclaim PepMap 100 C18 0.075 × 500 mm; 2.0 µm; Thermo Fisher Scientific	O- and N-linked glycopeptides recombinant human erythropoietin	80% ACN with 0.1% FA/ 0.1% FA	[55]
	Acclaim PepMap 100 C18 0.075 × 250 mm; 2.0 µm; Thermo Fisher Scientific	Recombinant SARS-CoV-2 spike protein expressed in the HEK 293 cell	ACN with 0.1% FA/ 2% ACN with 0.1% FA	[62]
	Aeris WIDEPORE XB-C18 2.1 × 150 mm; 3.6 µm; Phenomenex	hCG	90% ACN with 0.1% FA/ 0.1% FA	[54]
	Acquity UPLC Peptide BEH C18 0.075 × 150 mm; 1.7 µm; Waters Corporation	Sex hormone binding globulin, hemopexine, haptoglobin	ACN with 0.1% FA/ 2% ACN with 0.1% FA	[42]
Hydrophilic interaction liquid chromatography	cHiPLC HALO HILIC 0.075 × 150 mm; 2.7 µm; Eksigent	Hemopexin from human plasma	ACN with 0.1% FA/ 2% ACN with 0.1% FA	[48]
	SeQuant ZIC-HILIC 2.1 × 150 mm; 3.5 µm; Merck	A1GP and IgG standard from human serum	ACN/ACN/ammonium acetetate (50%/100%/100 mM)	[33, 34]
	SeQuant ZIC-HILIC 2.1 × 150 mm; 3.5 µm; Merck	Hemopexin and IgG standard from human serum	ACN with 0.1% FA/ 0.1% FA	[23]
	SeQuant ZIC-HILIC 2.1 × 150 mm; 3.5 µm; Merck	*O*-glycopeptides of caseinomacropeptide	ACN with 0.1% FA/ 0.1% FA	[49, 66]
	SeQuant ZIC-HILIC 2.1 × 150 mm; 3.5 µm; Merck	RNase B, Trastuzumab, hFibrinogen, CTLA4-Ig	sets of mobile phases with different ion-pairing reagents*	[67]
Hydrophilic interaction liquid chromatography	SeQuant ZIC-cHILIC 2.1 × 150 mm; 3.0 µm; Merck	RNase B, Trastuzumab, hFibrinogen, CTLA4-Ig	sets of mobile phases with different ion-pairing reagents*	[67]
	SeQuant ZIC-pHILIC 2.1 × 150 mm; 5.0 µm; Merck 4.6 × 50 mm; 5.0 µm; Merck	RNase A and RNase B	ACN with 10 mM $HClO_4$/ 10 mM $HClO_4$	[68]
	Acquity UPLC Glycan BEH Amide 2.1 × 150 mm, 1.7 µm; Waters Corporation	RNase B, Trastuzumab, hFibrinogen, CTLA4-Ig	Sets of mobile phases with different ion-pairing reagents*	[67]

Table 1 (continued)

	Column, column dimensions and manufacturer	Analyte	Mobile phase composition	References
	TSKgel Amide-80 2.0×150 mm; 3 µm; Tosoh Bioscience	RNase A and RNase B	ACN with 10 mM $HClO_4$/ 10 mM $HClO_4$	[68]
	XBridge BEH amide 3.0×150 mm; 2.5 µm; Waters Corporation	RNase A and RNase B	ACN with 0.05% TFA/ 0.05% TFA	[69]
	AdvanceBio Glycan Mapping 2.1×150 mm; 2.7 µm; Agilent Technologies	RNase A and RNase B	ACN with 0.05% TFA/ 0.05% TFA	[69]
	Acquity UPLC Glycan BEH Amide 2.1×150 mm; 1.7 µm; Waters Corporation	mAb	ACN with 100 mM ammonium formate/10 mM ammonium formate (pH 4.5)	[47]
	Acquity UPLC Glycan BEH Amide 2.1×150 mm; 1.7 µm; Waters Corporation	IgG and hemopexin standard from human plasma	ACN with 0.1% FA/ 0.1% FA	[23]
	Acquity UPLC Glycan BEH Amide 2.1×100 mm; 1.7 µm; Waters Corporation	PSA	90% ACN with 10 Mm ammonium formate/10 mM ammonium formate	[25]
Hydrophilic interaction liquid chromatography	HALO® penta-HILIC 0.075×150 mm; 2.7 µm; Advanced Materials Technology	Hemopexin standard from human plasma	ACN with 0.1% FA/ 2% ACN with 0.1% FA	[21]
	HALO® penta-HILIC 2.1×150 mm; 2.7 µm; Advanced Materials Technology	IgG and hemopexin standard from human plasma	ACN with 0.1% FA/ 0.1% FA	[23]
	HALO® penta-HILIC 2.1×150 mm; 2.7 µm; Advanced Materials Technology	Bovine fetuin	ACN/ 5% ACN with 50 mM ammonium formate	[24]
	ACE HILIC-A 2.1×100 mm, 1.7 µm; Advanced Chromatography Technologies	IgG standard from human plasma	ACN with 0.1% FA/ 0.1% FA	[43]
	ACE HILIC-B 2.1×100 mm, 1.7 µm; Advanced Chromatography Technologies	IgG standard from human plasma	ACN with 0.1% FA/ 0.1% FA	[43]
	ACE HILIC-N 2.1×100 mm, 1.7 µm; Advanced Chromatography Technologies	IgG standard from human plasma	ACN with 0.1% FA/ 0.1% FA	[43]
Porous graphitized carbon	HyperCarb 4.6×100 mm; Shandon Scientific	Fetuin	ACN with 0.1% TFA/ 0.1% TFA	[74]
	HyperCarb 6.4×100 mm; Shandon Scientific	Fetuin	ACN with 0.1% TFA/ 0.1% TFA	[75]
	HyperCarb 4.6×100 mm; Shandon Scientific	RNase B	ACN/water	[76]
	HyperCarb 0.18×100 mm, 5.0 µm; Thermo Fisher Scientific	Mucin-type O-linked glycopeptides	ACN with 0.1% TFA/ 0.1% TFA	[78]
	HyperCarb 1.0×150 mm; 5.0 µm; Thermo Fisher Scientific	RNase B, bovine fetuin, asialofetuin, A1GP from human plasma and murine IgG1	50% ACN with 25 mM ammonium acetate and 1.25% aqueous ammonia solution/25 mM ammonium acetate with 1.25% aqueous ammonia solution	[86]

Table 1 (continued)

	Column, column dimensions and manufacturer	Analyte	Mobile phase composition	References
	PGC (0.075 × 150 mm; 5.0 µm)	*N*- and *O*-glycopeptides of bovine lactoferrin, bovine kappa casein and bovine fetuin	90% ACN/3.0% ACN with 0.1% FA	[79]
	PGC (0.075 × 43 mm; 5.0 µm)	RNase B, human plasma vitronectin, PSA, mAb and darbepoetin alfa	90% ACN with 0.5% FA/ 3% ACN with 0.1% FA	[82]
	PGC (0.075 × 150 mm; 5.0 µm)	RNase B, IgG standard from human plasma, bovine lactoferrin and bovine κ-casein	90% ACN with 0.1% FA/ 3.0% ACN with 0.1% FA	[84]
	PGC (0.075 × 150 mm; 5.0 µm)	RNase B, bovine κ-casein and human serum	90% ACN with 0.1% FA/ 3.0% ACN with 0.1% FA	[85]
	Activated graphitized carbon (0.075 × 43 mm; 5.0 µm)	RNase B, bovine fetuin and horseradish peroxidase	97% ACN with 0.1% FA/ 3% ACN with 0.1% FA	[80]
Multi-dimensional chromatography	RP-HILIC (Jupiter C18 × TSKgel Amide-80) C18: 0.15 × 800 mm; 3.0 µm; Phenomenex HILIC: 0.15 × 800 mm; 5.0 µm; Tosoh Bioscience	Bovine serum albumin, RNase B, and horseradish peroxidase	97.5% ACN with 0.5% FA/ 2% ACN with 0.5% FA	[92]
	RP-PGC (Jupiter C18 × HyperCarb) C18: 0.15 × 150 mm; 3.0 µm; Phenomenex PGC: 0.15 × 150 mm; 5.0 µm; Thermo Fisher Scientific	RNase B	98% ACN with 0.5% FA/ 2% ACN with 0.5% FA	[93]
	RP-PGC (PepMap™ × HyperCarb) C18: 0.075 × 300 mm; 3.0 µm; Thermo Fisher Scientific	Bovine serum albumin and RNase B	84% ACN with 0.1% FA/ 0.1% FA	[94]
	PGC-RP (HyperCarb × Jupiter C18) HyperCarb: 0.15 × 150 mm; 3.0 µm; Thermo Fisher Scientific C18: 0.15 × 150 mm; 3.0 µm; Phenomenex	*Saccharomyces cerevisiae* cell lysates and from the plasma of *Macaca fascicularis*	pH 2: 98% ACN/2% ACN with 0.5% FA pH 10: 90.2% ACN in 2 mM ammonium formate/2% ACN in 20 mM ammonium formate	[95]
	RP-PGC (PepMap™ × HyperCarb) C18: 0.075 × 150 mm; 2.0 µm; Thermo Fisher Scientific PGC: 0.050 × 150 mm; 3.0 µm; Thermo Fisher Scientific	Human fibrinogen, bovine fetuin and IgG3 from human plasma	80% ACN with 0.1% FA/ 0.1% FA	[96]

IgG immunoglobulin G, *ACN* acetonitrile, *FA* formic acid, *A1GP* α1-acid glycoprotein, *hCG* human chorionic gonadotropin, *CTLA4-Ig* cytotoxic T-lymphocyte-associated protein 4, *RNase A* and *B* ribonuclease A and B, *ACN* acetonitrile, *TFA* trifluoroacetic acid, *A1GP* α1-acid glycoprotein, *RNase A* and B ribonuclease A and B, *PSA* prostate-specific antigen, *mAb* monoclonal antibody, *ACN* acetonitrile, *RNase A* and *B* ribonuclease A and B, *A1GP* α1-acid glycoprotein, *ACN* acetonitrile, *FA* formic acid

*The composition of the tested mobile phases are described in the publication [67]

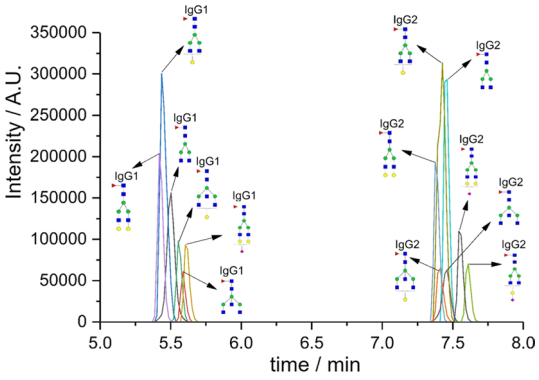

Fig. 1 Separation of human IgG standard on reverse phase C18 BEH column. Symbols: ■, *N*-acetylglucosamine (GlcNAc); ●, Mannose (Man); ○, Galactose (Gal); ▶, Fucose (Fuc); ◆, Sialic acid. These symbols are used thorough the whole review. Reprinted and edited with permission from Ref. [43]

(*N*-acetyllactosamine and fucose) did not influenced the retention to a large extent. Contrarily, in case of glycopeptides with sialic acid, peak broadening and enhanced retention times were observed. This behavior can be explained by the presence of active sites on the column that retain the acidic glycans. Another explanation for this phenomenon was proposed by Wang [52], who suggested that the increased retention of sialylated glycopeptides might be caused by the neutralization of negatively charged sialic acid by the positive charge of the peptide, resulting in stronger binding to the stationary phase. The same phenomenon was observed by Camperi and his co-workers [54] who characterized the human Chorionic Gonadotropin protein (hCG), a hormone specific to the human pregnancy, using an Aeris WIDEPORE XB-C18 column (2.1 × 150 mm; 3.6 µm). Their results showed enhanced retention times with increasing number of sialic acids.

Kozlik et al. [42] showed the dependence of relative retention times of the glycoforms of sex hormone binding globulin, hemopexine, and haptoglobin on the number of neutral monosaccharides unites. The glycopeptides were separated on Acquity Ultra-Performance Liquid Chromatography (UPLC) Peptide BEH C18 nano-column (0.075 × 150 mm; 1.7 µm) while different glycoforms were prepared by enzymatic digestions. They observed that fucose provided a less significant retention shift for larger glycans (comparing bi- tri-, and tetra-antennary forms). The effect of galactose and *N*-acetylglucosamine was examined, too. After degalactosylation of the glycopeptides there was a significant shift in retention times, most probably due to the different polarity of galactose and *N*-acetylglucosamine (galactose is more polar than *N*-acetylglucosamine). The overlaid chromatograms of the glycopeptide of haptoglobin and the dependence of relative retention time on the number of monosaccharides units is shown in Fig. 2.

Although RP-LC is not primarily used for isomer separation, Ji et al. [55] were able to separate the sialylated isomers of O- and N-linked glycopeptides of recombinant human erythropoietin. The measurements were carried out on an Acclaim PepMap™ C18 rapid separation liquid chromatography column (0.075 × 500 mm; 2.0 µm). The baseline separation of monosialylated isomers of *O*-glycopeptide (linkage either on the *N*-acetylgalactosamine or on the galactose) was achieved at 60 °C column temperature. They also separated the *N*-glycopeptides of α1-acid glycoprotein (A1GP) from human plasma, which are highly sialylated. Interestingly, in case of the sialylated glycopeptides with hydrophobic peptide backbone, the retention was prolonged at higher column

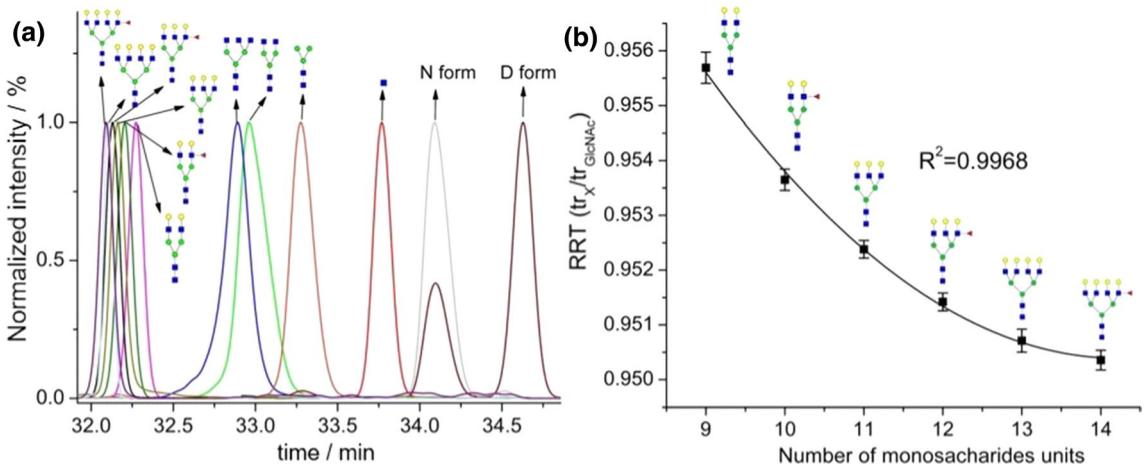

Fig. 2 The overlaid chromatograms of the glycopeptide of haptoglobin (**A**) and the dependence of relative retention time on the number of monosaccharides (**B**). Reprinted and edited with permission from Ref. [42]

temperatures while the opposite effect was observed for the more polar peptide backbone.

Recently, Zhong's research team [56] used linkage-specific derivatization of sialic acids of human A1GP and bovine fetuin glycopeptides. The separation was carried out on Acclaim PepMap™ 100 C18 column (0.075 × 150 mm; 2.0 µm). The derivatized sialylated glycopeptides eluted before the nontreated glycopeptides, due to the elimination of negative charges of sialic acid. In addition, the signal intensity of sialylated glycopeptides in MS was enhanced. The linkages of sialylated glycopeptides (either α2,3- or α2,6-linkage) were identified thanks to the mass difference between the derivatized isomers.

Since it has been proved that the spike protein and the receptors of the virus causing severe acute respiratory syndrome (SARS-CoV-2) are highly glycosylated, several papers on their characterization have been published [57–61]. All these papers employed RP chromatography before MS/MS. Sanda et al. [62] identified 17 N-glycosylated and 9 O-glycosylated peptides of the spike protein carrying complex, hybrid and high-mannose glycans. The separation was carried out on a C18 PepMap™ column (0.075 × 250 mm; 2.0 µm). The retention times of *O*-glycoforms were in agreement with trends observed in previously published papers [42, 48].

Hydrophilic interaction liquid chromatography

In contrast to RP-LC, HILIC is a more powerful technique for separation of glycopeptides, as it has the ability to retain highly hydrophilic analytes. HILIC employs a polar stationary phase, but the mobile phase is similar to that used in RP-LC [63]. In case of HILIC, the retention of glycopeptides is driven by a combination of partitioning and adsorption processes occurring between an acetonitrile-rich mobile phase and a thin water layer immobilized on a polar stationary phase [21, 48, 64, 65]. In recent years, several HILIC columns with various stationary phase modifications have been introduced. The ones that have already been used for separation of glycopeptides are summarized in Table 1.

Kozlík et al. [48] optimized and compared the separation of glycopeptides of hemopexin in RP-LC and HILIC mode. The HILIC separation was carried out on a cHiPLC HALO HILIC column (0.075 × 150 mm; 2.7 µm), which contains bare silica stationary phase. They observed that, unlike in RP-LC, in HILIC mode with the increasing polarity of glycans attached to the same peptide backbone the retention increased.

In case of stationary phases containing zwitterionic sulfoalkylbetaine functional groups attached to porous silica (ZIC-HILIC columns) electrostatic repulsion may occur between the negatively charged sulfobetaine functional group and the partly negatively charged sialic acid residues. This phenomenon was observed by Takegawa's research team who used a ZIC-HILIC column (2.1 × 150 mm; 3.5 µm) for the separation of sialylated *N*-glycopeptides of A1GP from human plasma [33] and human serum IgG [34]. A column with the same properties was used by both, Molnarova et al. [23] (separation of glycopeptides of hemopexin and IgG) and by Hernandez-Hernandez (separation of *O*-glycopeptides of caseinomacropeptide) [49, 66]. Both research groups observed a decreased retention time of sialylated glycoforms due to the presence of electrostatic repulsion between the stationary phase and the sialylated glycopeptide.

Furuki and Toyo'oka [67] investigated the effect of ion-pairing reagents in the mobile phase. The separation of glycopeptides was carried out on three different columns: BEH amide, ZIC-HILIC and ZIC-cHILIC (zwitterionic stationary phase with phosphorylcholine functional group) columns. They discussed the retention mechanism based on the ion-pairing reagents used and the given stationary phase. Generally, they observed a decreased retention of glycopeptides derived from RNase B, trastuzumab, hFibrinogen, and CTLA4 Ig when the hydrophobicity or concentration of anionic ion-pairing reagents (trifluoroacetic acid, pentafluoropropionic acid, heptafluorobutyric acid, nonafluorovaleric acid) increased. On the other hand, cationic ion-pairing reagents decreased retention times of sialylated glycopeptides.

Pedrali and her co-workers [68] compared the separation of intact glycopeptides of ribonuclease A (RNase A) and B (RNase B) on a TSKgel Amide-80 (2.0 × 150 mm; 3.0 µm) column and on a polymeric ZIC-*p*HILIC (2.1 × 150 mm and 4.6 × 50 mm; 5.0 µm) column. The mobile phase was composed of acetonitrile and water, both containing 10 mM $HClO_4$, the detection was carried out photometrically at 210 nm. According to the publication, better results were obtained in case of the amide functionalized stationary phase (the exact results of the separation on the ZIC-*p*HILIC column are not provided by the authors). They also studied the influence of column temperature on the separation and observed prolonged retention times, sharper and more symmetrical peaks at 50 °C than at 25 °C. Based on this research, Tengattini's group [69] tested two other amide columns, namely XBridge BEH amide (3.0 × 150 mm; 2.5 µm) and AdvanceBio Glycan Mapping (2.1 × 150 mm; 2.7 µm) for separation of RNase A and B glycopeptides. Since they used a UV–MS detection, the mobile phase consisted of acetonitrile and water, both with the addition of trifluoroacetic acid. The three amide stationary phases showed similar selectivity, but the AdvanceBio Glycan Mapping and XBridge BEH amide columns showed better separation performance than the TSKgel Amide-80. The Acquity UPLC Glycan BEH Amide column packed with amide sorbent

(2.1 × 150 mm; 1.7 µm) was also used by the research team of Gilar [47] for separation and glyco-profiling of several glycopeptides. They observed that glycopeptides interacted more strongly with the stationary phase and were successfully separated from the non-glycosylated peptides.

HILIC is not only a powerful technique for the separation of glycopeptides but is also suitable for the separation of their isomers. Most of the studies used a HALO® penta-HILIC column for glycopeptide isomer separation. This column contains five hydroxyl groups on the bonded ligand [21–24]. Molnarova and Kozlik [23] compared three different HILIC stationary phases, namely HALO® penta-HILIC, Glycan BEH Amide and ZIC-HILIC, in the separation of hemopexin and IgG glycopeptides and their isomers. The study focused on the separation of position isomers (core or outer arm) of monofucosylated glycans as well as on the monosialylated glycans with different branch position of sialic acid (unbranched α6-antenna or the branched α3-antenna with β2- or β4-branching) of hemopexin. In case of IgG, only one glycan isomer was observed, namely the linkage isomer of monogalactosylated bi-antennary glycan (attached either to α3- or α6-antenna). The results showed that the best separation of core and outer arm fucosylated hemopexine and the monosialylated hemopexin was achieved on the HALO® penta-HILIC column which was able to baseline separate the glycan isomers of hemopexin, while the IgG glycan isomer was only partly separated. The worst separation was achieved on the ZIC-HILIC column, and the Glycan BEH Amide column stood in between. The effect of the column temperature on the isomer separation was studied, too. In most cases, the resolution worsened with an increase in temperature.

The glycan BEH Amide column (2.1 × 100 mm; 1.7 µm) was also used by van der Burgt et al. [25] who separated the trypsin and ArgC digested sialylated glycopeptides of prostate-specific antigen (PSA) proteoforms. The composition of the mobile phase was optimized while the best separation was achieved using water and acetonitrile with 10 mM formic acid. The pH of the mobile phase did not affect the separation, on the other hand, the retention time of glycopeptides slightly decreased with increasing pH. In most cases, the buffer concentration did not affect the retention, however, it influenced the signal intensity (higher concentration of the buffer lowered the intensity). The linkage isomers of sialylated glycopeptides (either α2,3- or α2,6-linkages) were identified by exoglycosidase treatment by Sialidase S or A.

A recently developed HILIC columns introduced by Advanced Chromatography Technologies (ACE) containing different stationary phases (HILIC-A: unfunctionalized silica, HILIC-B: aminopropyl functionalized silica, HILIC-N: polyhydroxy functionalized silica) were compared with C18 column in the separation of human IgG glycopeptides. Among the HILIC columns, HILIC-A and HILIC-B showed a mixed-mode separation character. In case of HILIC-B column, an enhanced retention was observed because of the electrostatic attraction between the positively charged aminopropyl groups of the stationary phase and the partially negatively charged carboxylic acids of the peptide backbone. Moreover, in case of the sialylated glycopeptides, the retention increased significantly. On the other hand, in case of HILIC-A column, the lowest retention was observed probably because of the electrostatic repulsion between the partly dissociated silanol groups of the stationary phase and the three partly negatively charged carboxylic acids of the peptide backbone [43].

Porous graphitized carbon

Another option for glycopeptide separation is to use PGC that has unique properties as it has the power to separate both, hydrophilic and hydrophobic analytes. In PGC, the stationary phase consists of fully porous and spherical particles, while the mobile phase is a mixture of water (or buffer) and organic solvent (acetonitrile, methanol) with a possible addition of an organic modifier (formic acid, trifluoroacetic acid, ammonium acetate) [70–72].

The retention of the polar (hydrophilic) analytes is driven by a mechanism known as *polar retention effect of the graphite* (PREG). The more polar the analytes are, the higher affinity they have toward the graphite surface, resulting in longer retention, whereas in case of non-polar solutes, hydrophobic interactions play a key role [71]. Moreover, due to the surface planarity of PGC stationary phase, the 3D structure of the analytes can also influence the retention [64, 73].

To the best of our knowledge, PGC was first used for glycopeptide separation by Davies et al. [74, 75] who separated the glycopeptides of fetuin on a HyperCarb column (Table 1). A year later, Fan and his research group [76] separated a pronase digested glycopeptides of RNase B on Shandon HyperCarb (4.6 × 100 mm) and Carbonex (4.6 × 100 mm) column. They observed that glycopeptides with a short amino acid sequence were not retained on C18 column. In contrast, they were successfully separated within 40 min on the PGC one. Additionally, they observed that the glycopeptide retention was influenced by both, the glycan composition and the peptide backbone. Glycopeptides with larger peptide backbone, but with same glycan composition, eluted later due to their higher hydrophobicity. On the other hand, glycopeptides with higher number of mannoses eluted earlier. In comparison, the addition of an amino acid residue to the peptide backbone influenced the retention more than the addition of a saccharide unit to the glycan structure.

In another study, Wagner-Rousset et al. [77] employed a PGC column (0.075 × 43 mm, 5.0 µm) for separation

of recombinant antibodies, however, this research rather focuses on the glycoform characterization by tandem mass spectrometry than on the chromatographic separation. Thaysen-Andersen and his co-workers [78] employed a HyperCarb (0.18 × 100 mm, 5.0 μm) column for the separation of mucin-type *O*-linked glycopeptides. They compared the separation with C18 column using the same gradient program in both cases. They observed a similar trend in elution of the glycopeptides: glycopeptides with *N*-acetylgalactosamine and galactose attached to the peptide eluted as the first ones, followed by the less polar glycopeptides carrying only *N*-acetylgalactosamine. The glycopeptides with longer peptide backbone eluted as the last ones. Comparing with C18 column, on the PGC, the retention was prolonged.

Nwosu's research team [79] carried out a simultaneous separation of *N*- and *O*-glycopeptides of bovine lactoferrin, bovine kappa casein and bovine fetuin (each digested by pronase) on a chip-based PGC column (0.075 × 150 mm; 5.0 μm). They were able to separate isomeric glycopeptides of both *N*- and *O*-glycopeptides (in total, 233 glycopeptides were identified in a single mixture). In case of *O*-glycopeptides, positional isomers with one sialic acid (attached either to hexose or to *N*-acetylhexosamine) were successfully separated and identified based on their MS/MS spectra. Another example of isomer separation was observed for the *N*-glycopeptides with eight mannoses where the mannose units can be attached by α1-2-, α1-3-, or α1-6-linkage.

Another work used a chip-based chromatography on an activated graphitized carbon column (0.075 × 43 mm; 5.0 μm) for the separation of different tryptic glycopeptides. Activated graphitized carbon is prepared from non-graphitic carbon by graphitization heat treatment that results in 3D hexagonal crystalline structure. Glycopeptides derived from RNase B and horseradish peroxidase (both having shorter peptide backbones) were better retained and separated on the activated graphitized carbon column than on the chip packed with C18 material. On the other hand, glycopeptides with larger peptide backbone were not detected or identified on the activated graphitized carbon column due to their higher hydrophobicity, but were successfully retained on the C18 column. Another difference was observed in the peak shapes. While in case of the activated graphitized carbon column, significant peak broadening was observed (the width of the broadest peak was 1.6 min), on the C18 column, the peaks were much narrower (the broadest peak width was 0.8 min) [80].

To overcome the difficulties with hydrophobic glycopeptides produced by tryptic digestion, several studies used nonspecific proteases. These nonspecific proteases, e.g., pronase or proteinase K, do not digest the glycopeptide in the proximity of the glycosylation site but digest the peptide backbone to a small amino acid sequences (< 4 amino acid) [81]. Hua et al. [82] utilized a mixture of proteases (porcine elastase, papain, porcine pepsin, pronase, proteinase K, subtilisin, and thermolysin) to digest glycoproteins prior to their separation on a chip-based PGC column. Each of these proteases produced the most abundant glycopeptides with peptide backbone consisting of no more than 5 amino acid residues. Thanks to the sufficiently small glycopeptides, they were able to show the ability of PGC column to separate glycopeptide linkage isomer of monogalactosylated bi-antennary glycan (earlier-eluting α6-linked and later-eluting α3-linked galactose) of infliximab with a short peptide backbone (NST). On the other hand, in case of the glycopeptide with the same glycan composition but longer peptide backbone (QYNST), the isomeric separation was not observed.

Although PGC is also a powerful stationary phase material for separation of glycopeptide isomers, it has worse robustness and reproducibility of resolution and retention time comparing with the separation on HILIC columns [83]. A chip-based PGC column (0.075 × 150 mm; 5.0 μm) was used for the separation of pronase digested *N*- and *O*-linked glycopeptides of RNase B, human IgG, bovine lactoferrin, and bovine κ-casein by Hua et al. [84]. They observed that polar analytes were strongly retained on the column. The addition of sialic acid to the bi-antennary glycopeptides with NST peptide backbone prolonged the retention by approximately 1.9 min, while the addition of a galactose did not influence the retention that significantly (approximately 0.3 min retention shift). Glycopeptides with short peptide moiety (NST) eluted earlier than the ones with longer peptide backbone (EEQYNST and EEQFNST) where the presence of two glutamic acids increased the overall polarity of the glycopeptide resulting in stronger retention on the PGC column. In addition, glycopeptides with the EEQYNST peptide backbone eluted after the glycopeptides with EEQFNST backbone because tyrosine is more polar than phenylalanine. The study also focused on the separation of glycopeptide isomers. Two isomers of O-linked glycans carrying *N*-acetylgalactosamine, galactose and sialic acid attached to the STVAT peptide backbone, which differed in the attachment of sialic acid were separated. In case of the earlier-eluting isomer, sialic acid was conjugated to the core galactose, whereas the glycopeptide with sialic acid attached to *N*-acetylgalactosamine eluted later. The glycopeptide isomers were identified based on their MS/MS spectra.

The research group of Nwosu [85] used the same analytical column and model glycopeptides, which were produced by in-gel nonspecific proteolysis digestion. They were able to separate the O-linked glycopeptides (mostly sialylated) of κ-casein with multiple glycosylation sites and achieved the separation of the isomers containing *N*-acetylgalactosamine, galactose and sialic acid. Additionally, the highly mannosylated glycopeptides of RNase B with different length of the peptide backbone were successfully separated. The utility

of the method was tested on a complex mixture of glycopeptides derived from crude bovine milk and human serum, suggesting that the in-gel nonspecific proteolysis digestion can be applied to biological fluids.

PGC was also used by Zhu and his co-workers [86] who investigated the effect of the mobile phase composition and column temperature on the isomer separation of glycopeptides of bovine fetuin, RNase B and A1GP from human plasma. The separation was carried out on HyperCarb column (1.0 × 150 mm; 5.0 µm) using basic mobile phase (pH 9.9) consisting of 25 mM ammonium acetate with 1.25% ammonium hydroxide (mobile phase A) and 50% acetonitrile with 25 mM ammonium acetate and 1.25% ammonium hydroxide (mobile phase B). There were separated the disialylated isomers of fetuin, which were assigned to have sialic acid with both α2-3 and α2-6-linkages, while the glycoforms with α2-6-linkage eluted before those with α2-3 linkage. They also observed isomeric separation of neutral bi-antennary glycopeptides of murine IgG1 with one terminal galactose (galactose attached to a different arm) and for highly mannosylated glycopeptides (different positions of mannoses).

Multi-dimensional chromatography

To enhance the number of separated glycopeptides and to improve the separation efficiency, combination of different stationary phases has been utilized. In case of multi-dimensional chromatography, there are some aspects of the separation that need to be take into account: (1) mobile phase compatibility of the used LC methods, (2) compatibility of the mobile phase with the used detector, (3) compatible column dimensions and flow rates, (4) sample transfer between the columns and injection volumes [87–91].

Lam et al. [92] used a RP-HILIC system to separate the glycopeptides of bovine serum albumin, RNase B, and horseradish peroxidase. The RP separation was carried out on a C18 column, while the HILIC column was packed with Amide-80 stationary phase (0.15 × 800 mm in both cases). They compared the retention of the studied glycopeptides on LC modes standalone, then in combined mode. The RP-HILIC system was able to separate the glycosylated and non-glycosylated peptides in a single run. To deal with the solvent incompatibly between RP (highly aqueous solvent) and HILIC (highly organic solvent), flow-splitting capillaries with constant-pressure solvent delivery were used.

In another work, the same research team combined RP-RP and RP-PGC for the separation of a standard mixture containing peptides, glycopeptides and glycans. The RP-RP system was mainly used for the peptide separation, whereas the RP-PGC was able to separate more hydrophilic glycopeptides and glycans. First, the sample was injected into the first RP column using a mobile phase with pH 2. The non-retained hydrophilic compounds were automatically injected to the PGC column. In case of the glycopeptides of RNase B, the main glycopeptide forms consisting of highly mannosylated glycoforms (five to nine mannoses) were separated in the RP-PGC system. Using only the RP column, these glycopeptides were not detected. The glycopeptides eluted in the order of decreasing polarity, the glycopeptide with nine mannoses eluted first and the glycopeptide with five mannoses eluted last. In case of glycopeptide with seven mannoses, isomeric separation was observed, too [93].

Lewandrowski and Sickmann [94] combined RP-PGC for the separation of bovine serum albumin and RNase B. For the RP separation, PepMap™ column was used and for the PGC separation a HyperCarb one (0.075 × 300 mm; 3.0 µm in both cases). Thanks to the combination of these methods, both hydrophilic peptides and glycopeptides were successfully separated. The PGC-RP column setup was used by Zhao's research team who separated *N*-glycopeptides from *Saccharomyces cerevisiae* cell lysates and from the plasma of *Macaca fascicularis* [95].

The pronase-treated glycopeptides of human fibrinogen, bovine fetuin and IgG3 from human plasma were separated on a RP-PGC system (C18: Acclaim PepMap™ 0.075 × 150 mm; 2.0 µm; PGC: in-house made HyperCarb material 0.050 × 150 mm; 3.0 µm). In one sample run, they were able to identify both *N*- and *O*-glycopeptides of fetuin and fibrinogen. The *N*-glycopeptides with short peptide backbone were not retained on the RP column, however, the presence of a sialic acid enhanced their retention. On the other hand, glycopeptides with short peptide backbone carrying bi- and tri-antennary mono- and disialylated glycans were successfully separated on the PGC column. Due to the large peptide backbone and small glycan moiety of *O*-glycopeptides, they were rather retained on the RP column than on the PGC. In addition, the characterization of a previously uncharacterized glycosylation of C_H3 domain of human IgG3 was performed [96].

Glycan separation

Detaching the glycans from the peptide backbone somewhat simplifies the analytical challenges connected with the macroheterogeneity (site occupance). In case of glycan separation and analysis, the N- and O-linked glycans are enzymatically or chemically detached from the peptide [97]. Most of the works use peptide: N-Glycosidase F (PNGase F) for cleaving the linkage between the N-linked glycans and the peptide [98–102]. Due to the lack of a universal releasing enzyme for O-linked glycans, for their deglycosylation reductive β-elimination with sodium hydroxide is used. However, it does not allow further modification

(e.g., derivatization, fluorescent or colorimetric labeling) [103, 104]. There are some studies, where nonreductive β-elimination was utilized, enabling further modification of the released glycans [105–107]. Analysis of individual glycans offers a great potential to elucidate their structural diversity, improve the detection of the low abundant ones and to study their role in disease development and progression [7–9, 108–112]. In this chapter, we focus on the separation of released glycans utilizing different LC approaches. In general, before the separation of glycans by any LC method their derivatization and/or labeling is usually needed. Zhou et al. compared different derivatization strategies for LC–MS/MS analysis of *N*-glycans, including 2-aminobenzamide (2-AB), procainamide (ProA), aminoxyTMT, RapiFluor-MS (RFMS) labeling, reduction, and reduction with permethylation [113]. The most important separation conditions for glycan separation are summarized in Table 2.

Reversed phase chromatography

Due to the high polarity of glycans, there is a need for their derivatization with a hydrophobic tag prior to their retention on C18 columns. In 2017, Vreeker and Wuhrer [114] published a review on the separation of glycans in RP-LC. Since this review summarizes all the achievements in glycan separation using RP-LC published before 2017, we only discuss the work published after 2017.

The oligosaccharides of human milk were analyzed by Porfirio et al. [117] who separated the permethylated glycans on a nanoflow C18 column (0.075 × 150 mm). Compared to other works separating human milk glycans [115, 116], they were able to identify more than 100 glycans and isomers (mostly fucosylated). Thanks to the MS/MS analysis of permethylated glycans, no further exoglycosidase digestion was needed to assign the glycan isomers.

The permethylated glycans of bovine RNase B, fetuin, mouse brain extracts, recombinant HIV gp120 were separated on an Acclaim PepMap™ C18 column (0.075 × 150 mm; 2 μm). The addition of Li^+ to the mobile phase enabled the baseline separation of isomeric *N*- and *O*-glycans. The advantage of addition of Li^+ to the mobile phase is that it simplifies the adduct heterogeneity and enhances cross-ring fragmentation to improve the identification of isomers [118]. As mentioned previously, the progression of several diseases can be monitored by determining the glycan composition of body fluids. The N-glycan profile of cerebrospinal fluids from patients with Alzheimer's disease was investigated. The permethylated glycans were separated on the Acclaim PepMap™ C18 column (0.075 × 150 mm; 2.0 μm). They investigated the differences in glycan composition of samples of male and female Alzheimer's patients and samples obtained from a healthy control group. They observed that fucosylated and bisecting glycans had higher abundance in the case of female patient samples, while high-mannose glycans were less abundant in both male and female patient samples [119]. Predicting the retention times of released glycans is helpful in structure elucidation. The research team of Gautam [120] utilized Glucose Unit Index (GUI) to predict the retention of permethylated glycans of RNase B and fetuin. The separations were carried out on both, C18 and PGC columns. Permethylated glucose units derived from dextrin were used as elution standards for the calculation of the GUI values. The advantage of the GUI usage lies in the ability to use normalized retention time values that are independent of the LC system. The evaluated method was also tested on real samples derived from human breast cancer cell lines. The intra- and inter-laboratory tests showed high reproducibility and reliability of the method, suggesting the potential of using GUI for automated glycan identification.

In the last few years, micro-array pillar nano-LC (μPAC) columns have been commercialized that have favorable properties like good reproducibility, durability, and low back pressure. Recently, Cho et al. [121] separated the permethylated N- and O-glycans of RNase B and fetuin on a 50 or 200 cm μPAC column (5.0 μm pillar diameter, 2.5 μm inter pillar distance, 18 μm pillar height, 50 or 200 cm bed length). In this work, they used a standard nano-LC Acclaim PepMap™ C18 column (0.075 × 150 mm; 2.0 μm), too. Different concentrations of acetonitrile in the mobile phase were tested on the separation of RNase B glycans showing that lowering the concentration from 100 to 80% improved the separation and the shapes of the peaks (Fig. 3). The same experiment was carried out for the separation of sialylated glycans of fetuin and its isomers. Comparing the μPAC column to a standard bed packed C18, the bed packed column was able to separate the glycan isomers more effectively than the μPAC column. Some improvement in isomer separation have been demonstrated on a 200 cm μPAC column. The advantage of μPAC column is the possibility of using higher flow rates, thus improving the peak sharpness and reducing the analysis time. On the other hand, higher flow rates resulted in loss of sensitivity.

Beside permethylation, glycans can be modified by other derivatization techniques including, 2-aminopyridine (PA)-tagging or fluorescent labeling by either 2-aminobenzamide (2-AB) or 2-aminobenzoic acid (2-AA) suitable for MS detection [122]. Most of the studies utilizing these derivatization techniques are summarized in the aforementioned review [114]. Suzuki et al. [123] used the 2-AB tag to differentiate between the sialylated glycan isomers of human A1GP. The separation was carried out on an InertSustain AQ-C18 column (2.1 × 150 mm) coupled simultaneously to MS and fluorescence detector. The two-step linkage-derivatization procedure resulted in mass difference Δ = 28.031 between α2,3- and α2,6-linked sialic acid allowing the distinction between the two isomers.

Table 2 An overview of glycan separation by different liquid chromatography approach. Columns, column dimensions, column manufacturers, analytes, mobile phase compositions and references are summarized

	Column, column dimensions and manufacturer	Analyte	Mobile phase composition	References
Reversed phase chromatography	Acclaim PepMap™ 100 C18 0.075 × 150 mm; Thermo Fisher Scientific	Permethylated glycans of human milk	80% ACN with 0.1% FA/ 2% ACN with 0.1% FA in 1 mM sodium acetate	[117]
	Acclaim PepMap™ C18 0.075 × 150 mm; 2 µm; Thermo Fisher Scientific	Permethylated glycans of bovine RNase B, fetuin, mouse brain extracts, recombinant HIV gp120	Proteomic buffer: 80% ACN with 0.1% FA/0.1% FA Low lithium buffer: 80% ACN with 0.1% AA containing 0.1 mM lithium acetate/0.1% AA containing 0.1 mM lithium acetate High lithium buffer: 80% ACN with 0.02% AA containing 1 mM lithium acetate/0.02% AA containing 1 mM lithium acetate	[118]
	Acclaim PepMap™ C18 0.075 × 150 mm; 2.0 µm; Thermo Fisher Scientific	Permethylated glycans of cerebrospinal fluid from Alzheimer's disease patients	ACN with 0.1% FA/0.1% FA	[119]
	Acclaim PepMap™ C18 0.075 × 150 mm; 2.0 µm; Thermo Fisher Scientific	Permethylated N- and O-glycans of RNase B and fetuin	ACN with 0.1% FA/2% ACN with 0.1% FA	[121]
	C18 no information given	Permethylated glycans of RNase B and fetuin, human blood serum and breast cancer cell lines	ACN with 0.1% FA/2% ACN with 0.1% FA	[120]
	µPAC columns 5 µm pillar diameter, 2.5 µm inter pillar distance, 18 µm pillar height, 50 or 200 cm bed length; PharmaFluidics	Permethylated N- and O-glycans of RNase B and fetuin	ACN with 0.1% FA/2% ACN with 0.1% FA or 80% ACN with 0.1% FA/2% ACN with 0.1%	[121]
	InertSustain AQ-C18 2.1 × 150 mm; GL Sciences	Human A1GP, transferrin and bovine fetuin tagged with 2-AB	20% ACN with 0.2% FA/0.2% FA	[123]
	Magic C18 AQ 0.075 × 150 mm; 5 µm; Tosoh Bioscience	Native and P2PGN derivatized glycans from human plasma	98% ACN with 0.2% FA/2% ACN with 0.2% FA	[125]
	T3 C18 2.1 × 150 mm; 1.7 µm; Waters Corporation	2-AB labeled N-glycans of IgG derived from mammalian species	ACN with 0.1% FA/ 0.1% FA	[133]

Table 2 (continued)

	Column, column dimensions and manufacturer	Analyte	Mobile phase composition	References
Reversed phase chromatography	Acquity UPLC Glycan BEH Amide 2.1×100 mm; 1.7 µm; Waters Corporation	2-AA labeled N-glycans of recombinant therapeutic glycoproteins	ACN/150 mM ammonium formate (pH 4.5)	[124]
	Acquity UPLC Glycan BEH amide 2.1×50 or 150 mm; 1.7 µm; Waters Corporation	RFMS labeled glycans of anticitrinin murine monoclonal IgG1, pooled human IgG, and bovine fetuin	ACN/50 mM ammonium formate (pH 4.4)	[128]
Hydrophilic interaction liquid chromatography	Acquity UPLC Glycan BEH amide 2.1×50, 100 or 150 mm; 1.7 µm; Waters Corporation	2-AB labeled glycans of RNase B, fetuin, and IgG	ACN/100 mM ammonium formate (pH 4.5)	[129]
	Acquity UPLC Glycan BEH amide 2.1×50 mm; 1.7 µm; Waters Corporation	N-glycans of infliximab labeled with RFMS	ACN/50 mM ammonium formate (pH 4.4)	[130]
	Acquity UPLC Glycan BEH amide 2.1×150 mm; 1.7 µm; Waters Corporation	2-AB labeled N-glycans of IgG derived from mammalian species	ACN/50 mM ammonium formate (pH 4.4)	[133]
	TSKgel Amide-80 2.0×250 mm; Tosoh Biosciences	2-AA labeled human plasma	ACN/50 mM ammonium formate (pH 4.4)	[127]
	TSKgel Amide-80 4.6×250 mm; 5.0 µm; Tosoh Biosciences	Native and derivatized glycans of mAbs and RNAse B	ACN/250 mM ammonium formate (pH 4.4)	[131]
	In house packed Amide column 0.075×250; 5 µm; Prozyme	DMT-MM derivatized haptoglobin and human plasma	ACN with 0.1% FA/0.1% FA	[132]
	SeQuant ZIC-HILIC 2.1×150 mm; 3.5 µm; Merck	Native and derivatized glycans of (mAbs) and RNAse B	ACN/34 mM AA (pH 3.0)	[131]
	SeQuant ZIC-HILIC 2.1×150 mm; 3.5 µm; Merck	2-PA derivatized glycans of A1GP and IgG from human serum	ACN/ACN/ammonium acetate (90%/50%/ 20, 5 or 100 mM)	[33, 34]
	SeQuant ZIC-HILIC 2.1×150 mm; 3.0 µm; Merck	2-AB labeled and reduced glycans of mAbs	ACN/0.1% AA	[136]
	Halo® Penta-HILIC column 2.1×150 mm; 2.7 µm; Advanced Materials Technology	ProA labeled N-glycan of bovine fetuin	ACN/5% ACN with 50 mM ammonium formate (pH 4.4)	[22]
Porous graphitized carbon	PGC 0.075×43 mm; 5.0 µm	Native N-glycans of human serum	90% ACN with 0.1% FA/3% ACN with 0.1% FA	[135]
	PGC 0.075×43 mm; 5.0 µm; Agilent Technologies	N-glycans derived from RNase B, fetuin, thyroglobulin, A1GP, and IgG (both from human serum)	10% ACN with 0.1% FA/0.1% FA or ACN/2% ACN containing 7.5 mM ammonium acetate (pH 8.4)	[102]

Table 2 (continued)

	Column, column dimensions and manufacturer	Analyte	Mobile phase composition	References
	PGC 0.32 × 100 mm; Thermo Fisher Scientific	Borohydride-reduced glycans of human IgG, commercial mAb expressed in CHO cells, anti-HIV antibody 4E10	80% ACN in 65 mM ammonium formate/65 mM ammonium formate (pH 3.0)	[138]
	PGC 0.15 × 100 mm; 5 µm; Thermo Fisher Scientific	O-glycans of porcin gastric mucin	ACN in 10 mM ammonium bicarbonate/water	[142]
	HyperCarb 0.075 × 150 mm; 5 µm; Thermo Fisher Scientific	Permethylated glycans of RNase B and fetuin, human blood serum, and breast cancer cell lines	ACN with 0.1% FA/2% ACN with 0.1% FA	[120]
	HyperCarb 2.1 × 150 mm; 5 µm; Thermo Fisher Scientific	2-AB labeled and reduced glycans of mAbs	ACN/0.1% AA	[136]
	HyperCarb 0.18 × 100 mm; Thermo Fisher Scientific	Reduced N-glycans of fibrinogen (derived from different species) and transferrin	ACN/65 mM ammonium formate (pH 3.0)	[137]
	HyperCarb 0.15 × 150 mm or 0.1 × 200 mm; 3.0 µm; Thermo Fisher Scientific	Native glycans of RNase B and fetuin	ACN with 0.1% FA/0.1% FA	[140]
	HyperCarb 0.075 × 100 mm; 5.0 µm; Thermo Fisher Scientific	Permethylated glycans of RNase B, fetuin, A1GP, human blood serum, and breast cancer cells	ACN with 0.1% FA/2% ACN with 0.1% FA	[141]
	HyperCarb 0.18 × 200 mm; 5.0 µm; Thermo Fisher Scientific	O-glycans of MUC1	ACN with 8 mM ammonium bicarbonate/water	[143]
	ProteCol HyperCarb 0.3 × 100 mm or 0.15 × 100 mm; SGE Analytical Science	Reduced O- and N-linked glycans isolated from mucosal surfaces and ovarian tissues	80% ACN in 10 mM ammonium bicarbonate/10 mM ammonium bicarbonate	[139]
Multi-dimensional chromatography	AEX × HILIC (TSKgel DEAE-5PW × TSKgel Amide-80 or SeQuant ZIC-HILIC AEX: 2.0 × 50 mm; 5.0 µm; Tosoh Biosciences Amide-80: 2.0 × 150 mm; 5.0 µm; Tosoh Biosciences ZIC-HILIC: 2.1 × 150 mm; 5.0 µm; Merck	2- PA derivatives of N-glycans of human serum	ACN/water/0.5 M ammonium acetate	[144]
	HILIC × PGC (Click-Maltose × HyperCarb) HILIC: 4.6 × 250 mm; 5.0 µm; Acchrom HyperCarb: 4.6 × 150 mm; 5.0 µm; Thermo Fisher Scientific	N-glycans of ovalbumin	HILIC: ACN with 0.1% FA/0.1% FA PGC: ACN/water	[145]

Table 2 (continued)

	Column, column dimensions and manufacturer	Analyte	Mobile phase composition	References
	HILIC × RP (Acquity UPLC Glycoprotein amide × RP PLRP-S) HILIC: 2.1 × 150 mm; 1.7 µm; Waters Corporation RP: 2.1 × 30 mm; 5.0 µm; Agilent Technologies	mAbs	HILIC: ACN/0.3% TFA RP: ACN/0.1% FA	[146]

RNase A and *B* ribonuclease A and B, *A1GP* α1-acid glycoprotein, *MUC1* mucin 1, *CHO* Chinese hamster ovary, *mAbs* monoclonal antibodies, *2-AB* 2-aminobenzamide, *2-PA* 2-aminopyridine, *AEX* anion-exchange, *ACN* acetonitrile, *FA* formic acid, *AA* acetic acid, *TFA* trifluoroacetic acid, *IgG* immunoglobulin G, *RNase A* and *B* ribonuclease A and B, *A1GP* α1-acid glycoprotein, *2-AB* 2-aminobenzamide, *P2PGN* 4-phenethyl-benzohydrazide, *ACN* acetonitrile, *IgG* immunoglobulin G, *RNase A* and *B* ribonuclease A and B, *A1GP* α1-acid glycoprotein, *mAbs* monoclonal antibodies, *RFMS* RapiFluor-MS, *2-AA* 2-aminobenzoic acid, *2-AB* 2-aminobenzamide, *2-PA* 2-aminopyridine, *DMT-MM* 4-(4,6-dimethoxy-1,3,5-triazin-2-yl)-4-methylmorpholinium chloride, *P2PGN* 4-phenethyl-benzohydrazide, *ProA* procainamide, *ACN* acetonitrile

Hydrophilic interaction liquid chromatography

HILIC is considered to be the best choice for glycan separation because of the polar stationary phases that it utilizes. It is able to separate both, native and modified glycans. The 2-AA labeled N-glycans of recombinant therapeutic glycoproteins (Enbrel®, Humira®, NESP®) were separated by Jeong et al. [124]. The labeled glycans were separated on Acquity UPLC Glycan BEH column (2.1 × 100 mm; 1.7 µm). The glycans eluted in order of increasing polarity and size. The results showed the differences between Humira® and NESP® glycan composition, while Humira® consists mostly of neutral bi-antennary and highly mannosylated glycan types, the glycans of NESP® are mostly highly sialylated tetra-antennary ones. The tri-antennary glycans eluted before the tetra-antennary ones. On the other hand, glycans with *N*-acetyllactoseamine eluted later than their sialylated tetra-antennary counterparts. In case of Enbrel®, the glycans were assigned to have bi-antennary neutral, mono-, and disialylated structures.

Walker's research team [125] compared the separation of *N*-linked glycans from human plasma, both native and derivatized with 4-phenethylbenzohydrazide (P2PGN), in RP and HILIC modes. In case of RP mode, Magic C18 AQ column was used, while the HILIC separation was carried out on TSKgel Amide-80 packed column (0.075 × 150 mm for both columns). In case of HILIC separation, the native glycans were sufficiently retained on the column, in contrast with the derivatized ones (after derivatization, the glycans become more hydrophobic, which decreases their retention). On the other hand, native glycans were insufficiently retained on the C18 stationary phase while the derivatized ones were successfully separated. Although HILIC was able to separate derivatized and native glycans, it was not able to detect as many analytes as the RP-LC method. The disadvantage of the HILIC separation was that the derivatized glycans and the glycans that remained untagged might have coeluted (in case of RP, only the derivatized glycans were retained). Also, in case of HILIC peak, broadening was observed. Another fact is, that while 42 derivatized glycans were detected in case of HILIC separation, additional 18 ones were identified using RP mode.

In another work, the same research team used the TSKgel Amide-80 (0.075 × 100 mm) column to compare different hydrophobic derivatization reagents used to increase the ion abundance of analytes in MS. The glycans derivatized with hydrazone formation reaction showed more than fourfold increase in the ion abundance. They observed that increasing the hydrophobicity of the tag decreased the retention of the glycans on the HILIC column. In addition, using more hydrophobic reagents (with two phenyl rings instead of one) further increased the ion abundance [126]. Ruhaak et al. [127] used the TSKgel Amide-80 (2.0 × 250 mm) column for the separation of 2-AA labeled glycans from human plasma.

Lauber et al. [128] separated the glycans of anticitrinin murine monoclonal IgG1, pooled human IgG, and bovine fetuin labeled with RFMS reagent. The reagent consists of *N*-hydroxysuccinimide carbamate reactive group, a quinoline fluorophore, and a basic tertiary amine, allowing both fluorescent and MS detection of the glycans. The samples were separated on Acquity UPLC Glycan BEH Amide column (2.1 × 50 or 150 mm; 1.7 µm). Thanks to the use of the RFMS labeling agent, the intensity of the low abundant glycans increased, allowing the detection of isobaric glycoforms of anticitrinin murine monoclonal IgG1 consisting of a bi-antennary digalactosylated glycan (the galactoses are attached either to the *N*-acetylgalactosamines individually or they are linked through an α-1,3 bond).

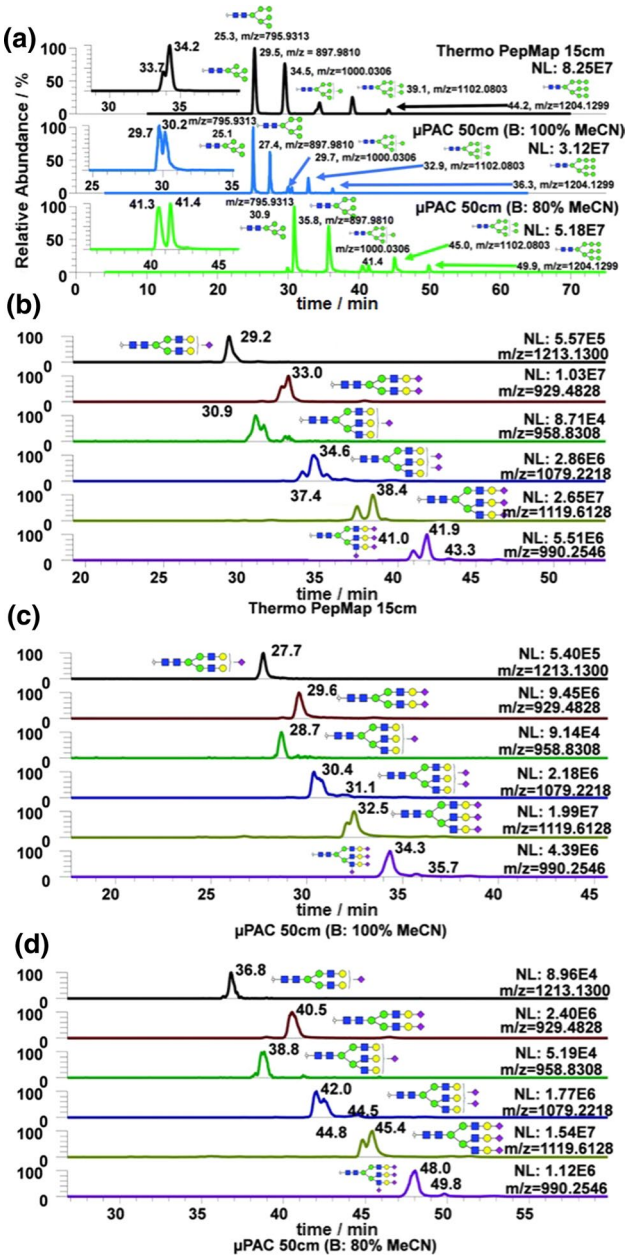

Fig. 3 Separation of permethylated glycans of RNase B (**a**) and bovine fetuin (**b**–**d**). Comparing the separation on the PepMap™ C18 and μPAC column. Lowering the concentration of acetonitrile from 100 to 80% improved the separation and shapes of the peaks. Reprinted and edited with permission from Ref. [121]

Ahn's research team [129] utilized the same column (Acquity UPLC Glycan BEH Amide, 2.1 × 50, 100, or 150 mm; 1.7 μm) for the separation of 2-AB labeled glycans of RNase B, fetuin, and IgG. The study compared the separation of the labeled glycans of fetuin on a column with 3 μm and 1.7 μm sorbent. In case of UPLC (1.7 μm sorbent), they observed an improvement in the separation of multiply sialylated glycans with positional isomers. The study also optimized the used gradient program. The results showed that the separation of glycans was affected by the initial mobile phase elution strength in the gradient program. Besides the effect of the initial elution strength, the effect of flow rate, column temperature, and column length were studied, too.

The separation of *N*-glycans derived from six batches of infliximab (biotherapeutics based on monoclonal antibodies) labeled with RFMS was also carried out on UPLC Glycan BEH Amide column (2.1 × 50 mm; 1.7 μm). The optimized method was able to separate the major glycan species within 5 min [130].

For profiling of both, the native and derivatized glycans of monoclonal antibodies (mAbs) and RNAse B the ZIC-HILIC column (2.1 × 150 mm; 3.5 μm) was used. The fluorescently labeled glycans were also separated on a TSKgel Amide-80 (4.6 × 250 mm; 5.0 μm) column. Comparing the separation of the neutral reduced glycans, the ZIC-HILIC column was able to separate the bi-antennary monogalactosylated isomers of mAbs that were only partly separated on the amide column. Then using the ZIC-HILIC column coupled to ESI–MS detection, they were able to identify less abundant glycans which was not achieved in case of amide column with fluorescent detection. In addition, the ZIC-HILIC column exhibited good retention time reproducibility and sensitivity, with no need of any additional labeling step [131].

The same ZIC-HILIC column was used by Takegawa's research team for the separation of 2-PA derivatized glycans of A1GP [33] and IgG [34] (both from human serum). The effect of ammonium acetate concentration in mobile phase on the retention of neutral and sialylated N-glycans was tested. Increasing the concentration from 5 to 20 mM increased the retention of the sialylated glycans (the retention of neutral glycans changed only slightly). This behavior can be explained by to the fact, that the increase in the electrolyte concentration decreases the electrostatic repulsion between the sialylated glycans and the stationary phase resulting in their enhanced retention. In this work, they also focused on the separation of sialylated isomers differing in the linkage of the sialic acid [33].

In their other work, they used the ZIC-HILIC column for the separation of 2-PA derivatized N-glycans of human serum IgG. The ZIC-HILIC column had the ability to separate the isomers of IgG differing in the linkage of galactose on the bi-antennary and bisecting glycan [34].

Tao et al. [22] used the Halo® Penta-HILIC column (2.1 × 150 mm; 2.7 μm) to separate the sialylated N-glycan isomers of bovine fetuin. The released glycans were labeled with ProA. Concerning retention times, the retention time difference between bi-antennary glycans with α2-3-linked sialic acid and those with α2-6-linked sialic acid is approximately 1.4 min. In case of larger glycans (tri-antennary), the

retention shift was not that significant. The cause of this may be that the retention was influenced by the overall size of the glycan rather than the effect of the linkage type.

Another work used a capillary column (0.075 × 250 mm) packed with amide bonded silica-based stationary phase for the separation of the tri-sialylated glycan isomers of haptoglobin and human plasma labeled with 2-AB (due to the fluorescence detection), which were further derivatized with 4-(4,6-dimethoxy-1,3,5-triazin-2-yl)-4-methylmorpholinium chloride (DMT-MM) in methanol. The combination of the HILIC and the derivatization method enabled the isomeric identification of the sialylated glycans, whereas the identification was mainly based on the mass shift between α2-3- and α2-6-linked sialic acids, which react with DMT-MM in different ways (glycans with α2-6-linkage produce methyl esters, while those with α2-3 linkage produce lactones), resulting in 32 Da mass difference. In addition, the derivatization by DTM-MM increases the hydrophobicity of sialylated glycans, thereby changing the selectivity of the HILIC separation [132].

Adamczyk's research team [133] compared HILIC, RP-LC, and CE for the elucidation of N-glycans of IgG derived from mammalian species labeled with 2-AB. The RP separation was carried out on a T3 C18 column (2.1 × 150 mm; 1.7 µm), while the HILIC separation utilized a Waters BEH Glycan column (2.1 × 150 mm; 1.7 µm). The electrophoretic separations were performed on a neutral coated capillary (50 µm id, 360 µm od, 60 cm total and 50 cm effective length). The CE instrument was equipped with laser-induced fluorescence detector (LIF). The abundances of glycans obtained by HILIC and CE-LIF were similar, whereas in case of RP-LC, it was difficult to compare due to the co-elution of many structures. In addition, the C18 column was not able to sufficiently retain highly hydrophilic sialylated glycans. The HILIC- and CE-based separations were also able to separate glycan isomers. This study gives a complete comparison including the advantages and disadvantages of each separation technique used.

Porous graphitized carbon

Released glycans, as well as glycopeptides, can be separated on columns packed with porous graphitized carbon material [134]. Hua et al. [135] identified and quantified the native N-glycans of human serum using a microfluidic chip packed with graphitized carbon (0.075 × 43 mm; 5.0 µm). The chip-based nano-LC/MS provided high sensitivity, minimal ion suppression, low sample consumption, and large instrumental dynamic range. On the PGC column, smaller glycans eluted earlier while complex glycans eluted later. They observed that the presence of sialic acid and core fucosylation increased the retention time. Retention was also enhanced by the addition of hexose and *N*-acetylhexosamine to the glycan structure. The increase in retention times was predictable only for the bi-antennary glycans. However, in case of tri-antennary ones, it was less foreseeable. In addition, the elution order of tri-antennary high-mannose type glycans was from the most complex to the less complex ones. This might have been caused by the different three-dimensional structures of tri-antennary glycans that can interact with both the stationary phase and mobile phase. They were able to separate and identify 300 N-linked glycans, including some isomers corresponding to structural and/or linkage isomers (e.g., bi- and tri-antennary disialylated and high-mannose glycans). The optimized method was used for glycan composition profiling of samples derived from prostate cancer patients.

Jmeian's research team [102] also utilized a chip-based PGC (0.075 × 43 mm; 5.0 µm) for the separation of N-glycans derived from RNase B, fetuin, thyroglobulin, human serum A1GP, and IgG. The glycans were online released by PNGase F monolithic reactor, which allowed fast and simultaneous release of neutral and sialylated glycans.

In another research, Mauko and his co-workers [136] compared the separation of 2-AB labeled and reduced glycans of mAbs on a ZIC-HILIC and PGC column. The HILIC separation was carried out on a SeQuant ZIC-HILIC column (2.1 × 150 mm; 3.0 µm) and the PGC separation on HyperCarb column (2.1 × 150 mm; 5.0 µm). The use of PGC column allowed the separation of isobaric glycans of mannosylated and galactosylated types. In addition, analysis using PGC column was able to identify low abundant glycans that were not observed on the ZIC-HILIC column (Fig. 4). On the other hand, PGC resulted in worse reproducibility of the retention times of sialylated glycans. In another study, two detection methods were compared, specifically fluorescence and MS. Although fluorescence-based detection is more used for glycan profiling, MS detection provides in-depth information about complex glycans, including their isomers.

To correct common retention time fluctuations on PGC columns, Pabst et al. [137] used an internal standard of bi-antennary glycan with two sialic acids. The *N*-glycans of fibrinogen (derived from different species) and transferrin were separated on the HyperCarb column (0.18 × 100 mm). The PGC column was able to separate the isomers of mono- and disialylated glycans, glycans with three or more *N*-acetyllactosamine units, and glycans with different linkages of fucose.

In another work, the same research team separated the glycans of IgG, different commercially available mAbs expressed in Chinese hamster ovary cells and the glycans of anti-HIV antibody 4E10 produced either in Chinese hamster ovary cells or in a human cell line. Using the PGC column (0.32 × 100 mm), they were able to separate the glycan isomers, including the bi-antennary and bisecting glycans

with different linkage of galactose, and the bi-antennary monosialylated ones. In contrast to the commercial mAbs, which lacked sialylated glycans, the preclinical anti-HIV mAb 4E10 consisted of a significant amount of sialylated and galactosylated glycans [138].

Karlsson et al. [139] separated the O- and N-linked glycans isolated from mucosal surfaces and ovarian tissues. The separation was carried out on both capillary and nano-LC ProteCol HyperCarb columns (0.3 × 100 mm column for capillary LC, or a 0.15 × 100 mm column for nano-LC). The MS detection was performed in the negative ionization mode allowing a simultaneous high sensitivity detection of neutral and negatively charged glycans.

She and co-workers [140] separated the native glycans of RNase B and fetuin on a HyperCarb packed column (0.15 × 150 mm or 0.1 × 200 mm; 3.0 µm). They were able to separate the isomers of high-mannose glycans, hybrid and complex sialylated glycans.

Zhou et al. [141] studied the effect of the column temperature on the separation of permethylated glycans of RNase B, fetuin, A1GP, and human blood serum on the HyperCarb PGC (0.075 × 100 mm; 5.0 µm). They observed that as the column temperature was increased, the retention of the glycans was enhanced, too. In addition, the results showed that at 75 °C (optimal temperature) multiple isomers of the model glycans were separated and identified. The optimized method was tested on breast cancer cells and different changes in the distribution of isomeric sialylated glycans were observed.

The O-glycans of porcine gastric mucin were separated by Jin et al. [142] using a PGC column (0.15 × 100 mm; 5 µm). The glycans were released by β-elimination and analyzed by ion mobility–MS. They were able to separate and identify the isomers of sialylated glycans which only differed in terminal *N*-acetylhexosamine (either β-*N*-acetylglucosamine or α-*N*-acetylgalactosamine), the neutral linear and branched glycan isomers (consisting of 2 hexoses and 2 N-acetylhexosamines) and the one with different fucose position.

Bäckström et al. [143] separated the O-glycans of MUC1 derived from different cancer cells on a HyperCarb column (0.18 × 200 mm; 5.0 µm). They observed different structures of O-glycans derived from different types of cancer cells, but all of them were sialylated. The glycans derived from breast cancer cells consisted mainly of sialylated core 1 structures (galactose attached to *N*-acetylgalactosamine), in case of the prostate cancer glycans core 2 structures with sialic acid dominated (galactose and *N*-acetylglucosamine attached to *N*-acetylgalactosamine), and in case of gastric cancer tissues both sialylated and fucosylated core 1 and core 2 structures were separated. In addition, the glycans derived from gastric cancer tissues exhibited highly α6-sialylated and branched galactosylated structures. The isomers differing in the position of both sialic acid and fucose attached to core 1 or core 2 were successfully separated.

Multi-dimensional chromatography

The advantages of multi-dimensional chromatography separation of glycans are the same as in the case of glycopeptide separation. However, there are only a few reports of its use.

The two-dimensional chromatography coupling anion exchange and HILIC columns was used by Deguchi et al. [144] for the separation of 2-pyridylamino derivated glycans of human serum. The HILIC separation was carried out either on the TSKgel Amide-80 (2.0 × 150 mm; 5.0 µm) or on the SeQuant ZIC-HILIC (2.1 × 150 mm; 5.0 µm) column. The separation on the anion-exchange column utilized diethylaminoethylene (DEAE) packed TSKgel DEAE-5PW (2.0 × 50 mm; 5.0 µm) column.

Cao's research team [145] used a combination of HILIC Click-Maltose (4.6 × 250 mm; 5.0 µm) and PGC HyperCarb (4.6 × 150 mm; 5.0 µm) column to purify the neutral N-glycans of ovalbumin. A total of 31 compounds (7 pairs of isomers), including high-mannose, hybrid, and multi-antenna asymmetric complex types were identified.

In another work, Stoll and his co-workers [146] developed a method combining RP and HILIC column for the separation of mAbs. In the first dimension, two Acquity UPLC Glycoprotein amide columns (2.1 × 150 mm; 1.7 µm) connected in series were used, while in the second dimension, a RP PLRP-S column (2.1 × 30 mm; 5.0 µm) was employed. The mobile phase consisted of 0.3% trifluoroacetic acid in water and acetonitrile (HILIC separation) and of 0.1% formic acid in water and acetonitrile (RP separation) while the detection was carried out at 280 nm photometrically. Three mAbs were studied, namely cetuximab, obinutuzumab, and atezolizumab. They observed high selectivity of the combined method for separation of heavily glycosylated cetuximab, whereas they were able to separate the main glycans (mostly bi- and tri-antennary hybrid types) and the isomeric form consisting of bi-antennary monogalactosylated glycan.

Capillary electrophoresis

Intact glycoprotein separation

There are several review articles and book chapters dealing with CE methods for glycoprotein analysis [147–150], the last one was published in early 2022. Nowadays, most CE glycoprotein analysis methods are coupled with MS detection as it has been proven a useful tool for analyzing intact glycoproteins in terms of glycosylation characterization. The use of MS brings some limitations to the choice

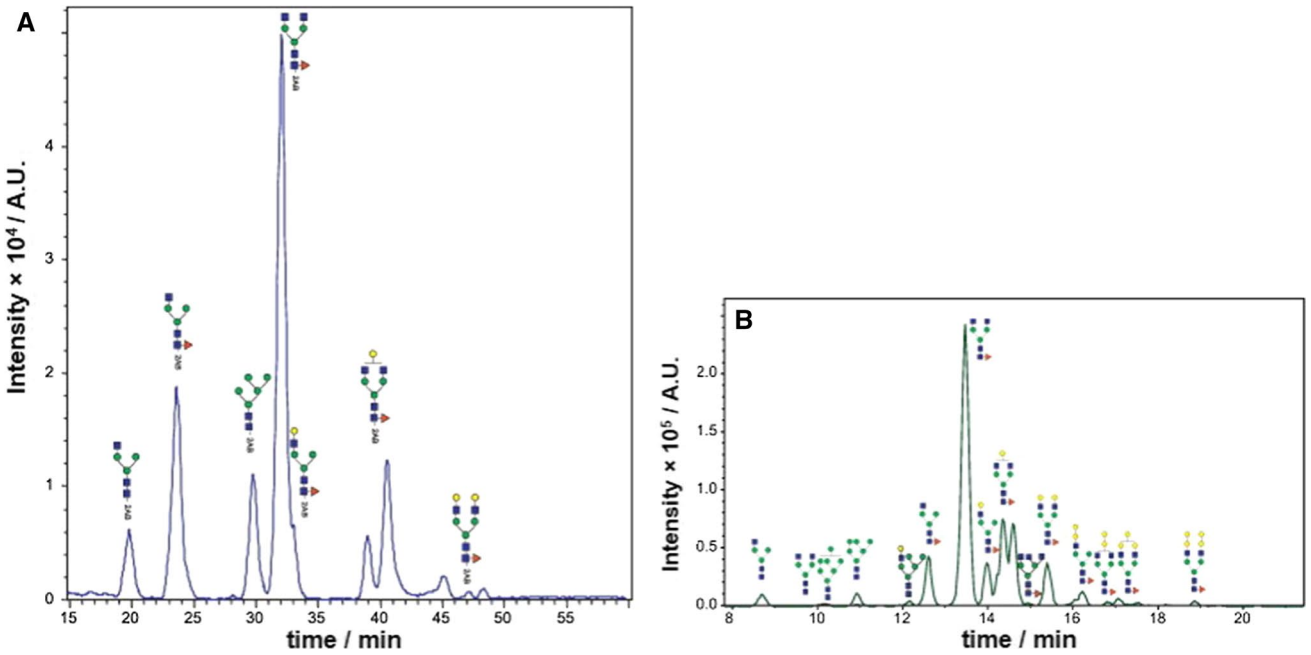

Fig. 4 Separation of 2-AB labeled glycans from mAb3 on ZIC-HILIC (**A**) and the neutral reduced glycans from mAb3 on PGC column (**B**) both coupled to ESI–MS. On the PGC column, low abundance glycans were observed that were not identified on the ZIC-HILIC column. Reprinted and edited with permission from Ref. [136]

of experimental conditions. The separation is performed in a relatively simple volatile background electrolyte (BGE) and there is no great variety in BGEs used. The capillary is usually coated with a coating agent prior to the analysis to avoid or minimize the adsorption of glycoproteins to the capillary wall and to control the velocity and direction of the electroosmotic flow (EOF) [150]. In this part of the review, we thus sort the methods by the type of the capillary coating used. Three types of capillary wall coatings are used for the CE characterization of intact protein glycosylation, i.e., coating with an anionic agent, such as polybrene/dextran sulfate double-layer, coating with a neutral agent, such as polyvinyl alcohol or polyacrylamide, and coating with a cationic agent such as polybrene.

The application of anionic wall coatings that generate a strong cathodic EOF is rather rare in the separation of intact glycoproteins. Sanz-Nebot et al. [151] presented a separation of human transferrin glycoforms in a permanently coated capillary. The separation was possible due to the differences in the sialic acid number and the size of the attached glycans. First, they tested cationic coating by a single polybrene layer which did not provide a sufficient separation. They thus used a second layer of dextran sulfate resulting in a permanent negative charge of the capillary wall leading to a pH-independent cathodic EOF. They used ammonium acetate buffer, pH 8.5 to assure the negative charge of glycoprotein isoforms. A CE–UV method was optimized and used for analyzing serum samples of four healthy volunteers and three patients with different types of congenital disorders of glycosylation (CDG). They were able to separate 7 glycoforms of transferrin, wherein glycoforms 0, 1, and 2 were not present in the samples obtained from healthy patients. The optimized CE–UV method was then coupled with MS detection to prove its future potential in CDG diagnosis after further optimization as the sensitivity of the CE–MS method was rather low and thus not all isoforms could be detected.

When the capillary is coated with a neutral agent, EOF is suppressed, and in combination with an acidic BGE (typically acetic acid), the glycoprotein isoforms are positively charged. Due to the low pH of the BGE, the dissociation of the acidic amino acid side chain groups and the sialic acid are suppressed. On the contrary, the basic amino acid side chain groups are protonated and thus glycoforms can be separated as cations. Haselberg et al. [152] utilized a CE-MS method for glyco-profiling of human interferon-β and human erythropoietin leading to the identification of 18 glycoforms and 80 isoforms of interferon-β and 74 glycoforms and 250 isoforms of erythropoietin. The isoforms were presented due to the presence of deamidation, succinimidation, oxidation, and/or acetylation of those glycoforms. They concluded that this methodology is suitable for the fast characterization of pharmaceutical proteins and thus it could be used in the quality control of pharmaceuticals. Moreover, it could be used for diagnostics and, after incorporation of an

appropriate pre-concentration technique, for doping control. The same group used commercially available coated capillary (hydrophobic layer/polyacrylamide double-layer coating) for characterization of mAbs used as therapeutics. They were able to determine glycosylated and clipped forms of antibodies which can be utilized in the determination of protein heterogeneity [153].

Lastly, a cationic wall coating generates a strong anodic EOF. In these cases, an acidic BGE is also used so that the glycoprotein isoforms are positively charged as mentioned previously. Ongay and Nesüss [154] were able to differentiate more than 150 isoforms of intact A1GP in human blood serum samples by CE-MS. They acknowledged the fact that combinations in the degree of sialyation, number of hexoses, and other minor modifications could lead to identical *m/z* values and thus subsequently performed an analysis of released glycans and of deglycosylated protein. Glycans were released from A1GP enzymatically (PGNase F) and then analyzed in their underivatized form by CE–MS in an uncoated silica capillary. Analysis of deglycosylated A1GP by CE–MS was performed under the same conditions as in the case of intact A1GP apart from the capillary coating as they coated the capillary with the neutral agent. That led to a faster analysis of deglycosylated protein due to the absence of sialic acid units. This complex approach was then used for the first time for the clinical studies of 16 different human A1GP samples.

Glycopeptide separation

In comparison with the intact glycoproteins, glycopeptides obtained from proteins by their proteolytic cleavage are less problematic analytes in terms of adsorption to the capillary wall and thus they can also be separated in uncoated bare silica capillaries. The main advantages of CE are the fast analysis, a small amount of sample needed, and high selectivity resulting for example from the use of online pre-concentration techniques. Kammeijer et al. [155] presented a CE-MS method for the differentiation between α2,3- and α2,6-sialylated glycopeptides, as the carboxylic group of sialic acid in each isoform has a different value of pK_A constant and thus exhibit different mobility in BGE. The separation took place in a bare fused silica capillary and the BGE was acetic acid at pH 2.3. They estimated the relative difference in pK_A values of α2,3- and α2,6-sialylated lactose with an internal standard-CE method, which was first proposed by Fuguet et al. [156], by calculating limiting and effective mobilities. They were able to identify 75 glycoforms by analyzing a tryptic digest of PSA with CE-MS, compared to MALDI-TOF–MS profiling, where 37 PNGase F released *N*-glycans were detected. The same group later showed the importance of the differentiation between α2,3- and α2,6-sialylated glycoforms for the development of a high-performance PSA glycomics assay as the α2,3-forms are thought to be present in aggressive types of prostate cancer. In addition to sialic acid linkage isoforms, they were able to determine the level of protein fucosylation. All of this has a high potential to improve the diagnosis of prostate cancer and possibly other types of cancer because a new biomarker with differently linked sialic acids can be discovered [157].

Amon et al. [158] performed CE-MS analysis of antithrombin tryptic digest in a bare fused silica capillary and in two differently coated capillaries in ammonium formate, pH 2.7, 5.0, or 8.0. They used a polybrene/dextran sulfate as a double-layer anionic coating, generating cathodic EOF, or polybrene as a cationic agent generating anodic EOF. The separation of glycopeptides in an uncoated capillary was insufficient as amino acid sequence coverage in peptide mapping was no more than 77% and based on the pH of BGE, 0 to 3 major glycopeptides were detected. In the case of polybrene coating, the coverage increased up to 81% and all 4 major glycopeptides with 2 minor glycoforms (monosialylated) were detected. Double-layer coating increased the amino acid coverage to 97%, all 4 major glycopeptides with 1 minor glycoform (fucosylated) were detected, monosialylated glycoforms were not detected. This developed method for glycopeptide mapping is thus competitive with the typically used RP-HPLC separation technique as the obtained data were in a good agreement.

To demonstrate the potential of CE, Zhang et al. [159] compared hydrodynamic and electrokinetic injection of A1GP glycoforms. They used a neutral agent, poly(ethylene oxide), to coat the capillary wall and acetate buffer, pH 4.2 containing 0.05% coating agent and 0.1% Brij 35. The 5-min sample stacking by − 5 kV brought an 11 000-fold increase in the loading capacity when compared to the hydrodynamic injection. The serum samples of healthy volunteers and patients with systemic lupus erythematosus were measured after acidic hydrolysis and desalting by CE-UV at 200 nm and 11 glycoforms were identified.

Glycan separation

Advances in glycan separations using CE have been summarized in a review published by Lu et al. in 2018 [160]. In this review, we thus focus on articles published since 2019. The main difficulty to be overcome when using CE for analysis of glycans released from glycopeptides and glycoproteins is the lack of readily ionized functional groups (except the carboxylic group present in the sialic acid). The second major problem when using CE with UV/Vis or fluorescence detection is the absence of chromophores and fluorophores that would provide sufficiently strong absorption or fluorescence.

Glycans are thus usually labeled by charged derivatization agents containing strong chromophores or fluorophores. The labels are usually negatively charged. The most frequently used label is definitely 8-aminopyrene-1,3,6-trisulfonic acid (APTS), other examples are 9-aminopyrene-1,4,6-trisulfonic acid (ANTS), and 2-AA. One of the research directions in the CE glycan analysis is thus aimed at the development of novel labeling procedures. Since this review focuses on separation part of the analysis, it is needless to say the choice of labeling agent significantly influences electrophoretic mobilities and thus separation of glycans, not only their detection.

Fomin et al. [161] introduced new fluorescent dyes for capillary gel electrophoresis with laser-induced fluorescence detection (CGE-LIF) analysis of glycans. The reactive dyes were based on phosphorylated 7,9-diaminoacridine derivatives with variable number of negative charges and the derivatized analytes showed higher mobilities then the APTS-labeled ones. The authors proved viability of the method by the separation of maltodextrin ladder and sialyllactose isomers in slab-gel electrophoresis format.

Khan et al. [162] used a new derivatization agent called Teal™. This label contains three sulfonic groups similarly to APTS. The authors reported on higher reactivity of this agent, which enabled its usage in lower excess over the analytes, resulting in significantly lower consumption of the dye than in the case of APTS. The initial experiments were performed in ammonium acetate buffer with 20% acetonitrile and 20% isopropanol as the BGE, nevertheless, frequent capillary flushing was necessary to regenerate the capillary surface. The BGE was thus replaced with ammonium hydroxide in 50% methanol, which not only provided a stable condition of the capillary wall but also significantly widened the separation window. Using this method, CE–LIF–MS analysis of a mixture of 9 high mannose and sialic acid glycans and 8 N-glycans commonly found in therapeutic mAbs was carried out. Glycans from both samples were baseline separated. They have proved the compatibility of the labeling with both detection techniques and reported the MS sensitivity comparable to APTS-labeled glycans.

The most used labeling procedure is based on reductive amination of reducing end of glycans with APTS, nevertheless, reductive amination is not the only reaction that can be used to introduce the aminopyrene-1,3,6-trisulfonic acid label to a glycan molecule. Krenkova et al. [163] compared the efficiency of glycan labeling using reductive amination and hydrazone formation reactions. They performed labeling of glycans released from RNase B and human IgG. They used the well-established protocol for APTS labeling using reductive amination while for the hydrazone formation-based derivatization, they used 8-(2-hydrazino-2-oxoethoxy)pyrene-1,3,6-trisulfonic acid (Cascade Blue hydrazide). Both resulting fluorescent labels contained the pyrene-1,3,6-trisulfonic acid motif differing only in the linkage connecting it to the glycan structure. They reported significantly higher labeling yield for hydrazone formation reaction. They ascribed the low labeling efficiency of reductive amination to competitive reduction of aldehyde functionality of the analytes to alcohol which hinders Shiff's base formation with APTS label.

Although glycans are usually labeled with negatively charged compounds, application of cationic labels can be beneficial in some cases. The same research group introduced new multi-cationic aminopyrene-based labeling tags. They derivatization agents were prepared from APTS by formation of sulfonamides with three tertiary amines in the structure. By further methylation they turned tertiary amines to quaternary ones with a permanent positive charge. They used fused silica capillary coated with linear polyacrylamide and 100 mM acetic acid as a BGE. The glycans labeled with the novel labels were separated under positive voltage polarity. They separated malto-oligosaccharides and N-glycans from bovine RNAse B and human IgG using CE-MS. However, they observed formation of side products during the labeling reaction thus the reaction procedure needs further optimization [164].

Kinoshita and Yamada [165] in their very recent review summarized the trends in modern sample preparation and chemical modification methods for the structural and quantitative glycan analyses together with their challenges and advantages. Further up-to-date information concerning the glycan labeling can be thus found there.

Novel approaches are introduced not only in glycan labeling. Detection sensitivity is one of the main challenges in CE-LIF glycomic analysis. Liénard-Mayor et al. [166] presented a novel strategy to improve detection sensitivity and peak capacity in CE-LIF analysis of APTS-labeled glycans. From the set of background electrolytes tested, they chose triethanolamine/citric acid and triethanolamine/acetic acid at high ionic strengths (up to 200 mM), which helped to create a large conductivity difference between sample zone and background electrolyte. This conductivity difference was used in electrokinetic pre-concentration strategy using large volume sample stacking. The high ionic strength also helped to suppress the EOF in bare silica capillary. Using this approach, they achieved a 200-fold signal enhancement. They demonstrated the applicability of the method on separation of N-glycans from human IgG and mapping of N-glycans from human serum for the diagnosis of CGD.

An interesting strategy to enhancing the sensitivity was presented by Shao et al. [167] who utilized an unexpectedly strong interaction between sulfonate groups of APTS-labeled glycans and Zr^{4+}-modified poly(ethylene glycol methacrylate phosphate-co-acrylamide-co-bis-acrylamide) monolith. The enriched sample was then offline transferred and analyzed by CE-LIF. Enrichment factors ranged from 9 to 24. The method was successfully applied to analysis

of N-glycans from RNAse B. Separation was performed in a bare silica capillary with lithium acetate buffer, pH 4.75 used as a BGE. The authors claimed that their enrichment method was more specific than commercial SPE columns packed with HILIC or PGC materials.

One of the assets of CE is the possibility to perform enzyme reactions or affinity interactions directly inside the capillary. Innovations from this area came in combination with the use of capillary nanogel electrophoresis [168]. This technique uses capillaries filled with nanogels composed of 1,2-dimyristoyl-*sn*-glycero-3-phosphocholine and 1,2-dihexanoyl-*sn*-glycero-3-phosphocholine phospholipids [169]. Nanogel is a non-Newtonian fluid, in which phospholipids self-assemble to form temperature-dependent morphologies. It has a low viscosity at lower temperature (i.e., below 20 °C) and a gel-like viscosity at a temperature of 25 °C and higher. It can thus be easily transported into and removed from the capillary at low temperature and serve as a gel separation matrix at higher temperatures. This feature enables formation of a stationary plug of an affinity agent in the inlet part of the capillary, which was utilized by Lu and Holland [170]. They performed electrophoretic experiments with stationary plugs of various lectins placed at the inlet part of the capillary. Peaks of N-glycans specifically interacting with the lectin used were then absent in the respective electropherograms. BGE pH was set to roughly match the p*I* of most lectins used, making sure the lectin zone would remain stationary. The method was used for IgG N-glycan profiling. Released N-glycans were labeled with APTS and separated in the nanogel using phosphate buffer, pH 6 as the BGE followed by LIF detection.

Another interesting application of capillary nanogel electrophoresis was reported by Bwanali et al. [171] who developed a method for analysis of N-glycans containing α2,6-linked sialic acid. The method integrated sequential enzymatic modification of sialylated N-glycans. It was validated using a tri-antennary N-glycan standard. The APTS-labeled N-glycans introduced to the capillary first passed through three enzyme zones. The first one contained α2-3-sialidase, the second one contained β1-3,4-galactosidase and the third one contained α2-3,6,8-sialidase. Migration through the first two zones resulted in cleavage of any α2,3-linked sialic acid (in the first zone) and penultimate galactose attached to the cleaved α2,3-linked sialic acid (in the second zone). This is represented by the first arrow in Fig. 5A. Migration through the third zone cleaved all remaining sialic acids, i.e., the α2,6-linked ones, which is represented by the second arrow in Fig. 5A. Since there was no further β1-3,4-galactosidase zone in the capillary, galactose residues linked to the cleaved α2,6-linked sialic acids remained in the glycan structure. As can be seen from Fig. 5B, when neutral galactose monomer is cleaved off, the resulting glycan possesses the same charge but a different size, which results in migration time shift during the subsequent separation in the nanogel matrix. The value of the shift is proportional to the number of galactose residues remaining in the glycan, and thus is proportional to the number of α2,6-linked sialic acids in the original structure. The method was validated by an experiment with only one enzyme plug of α2-3-sialidase (Fig. 5C). In this case, only α2,3-linked sialic acids were cleaved while all α2,6-linked ones and all galactose residues remained. The mobility thus increased with increasing number of negatively charged α2,6-linked sialic acid residues. Contrary to Fig. 5B, the more α2,6-linked sialic acids, the shorter migration time. From the relative peak areas, it can be seen that both approaches provided identical results. Separation was done in sodium acetate buffer, pH 5.0 as a BGE. The method was successfully tested on quantification of α2,6-linked sialic acids in structures of a complex *N*-glycan mixture released from A1GP. In this case, additional plugs containing specific lectins were introduced to the capillary inlet to capture glycans containing certain terminal monosaccharide residues and thus to provide additional structural information.

Due to their high specificity, lectins are relatively often part of glycomic protocols. Giron et al. [172] used CE-LIF of APTS-labeled N-glycans in combination with lectin micro-array and reported new non-invasive plasma and IgG glycomic biomarkers that provide information about time to HIV viral rebound and viral setpoint in two geographically distinct cohorts (Philadelphia and Johannesburg).

Although the above-mentioned nanogels represent a novel separation matrix for glycomic CE, capillary gel electrophoresis with laser-induced fluorescence detection (CGE-LIF) using classical gels is a well-established technique in this field. Commercial HR-NCHO gel buffer from Sciex which is usually used in a bare silica capillary is a very popular separation matrix. Mészáros et al. [173] utilized CGE-LIF with this gel for N-glycosylation profiling of pooled human serum samples from patients with lung cancer, patients with chronic obstructive pulmonary disease, comorbidity patients, and a healthy control group. They analyzed APTS-labeled glycans and defined a panel of 13 N-glycan structures as potential biomarkers with significant differences in abundance between the pathological and control samples. They also observed alterations in individual N-glycan subclasses, such as total fucosylation, degree of sialylation, and branching. The proposed biomarkers should help to diagnose and distinguish lung cancer and chronic obstructive pulmonary disease, which is vital as both diseases are treated in different ways.

Using the same separation gel, this group compared relative areas of 21 APTS-labeled N-glycans using machine learning-based data analysis, considering individual glycans as well as their subclasses, from serum samples of patients before and after lung tumor removal surgeries. They

modified the analysis procedure by implementing magnetic bead-mediated sample cleanup and pre-injection of a short plug of water before sample to focus the analyte zones. They were able to clearly distinguish alterations caused by the surgery, both positive and negative. They found correlation between glycosylation alterations and clinical parameters of the patients. They proposed N-glycosylation profiling to be used as a tool for monitoring of the effect of surgeries and the process of recovery [174].

Torok et al. [175] used the HR-NCHO gel for N-glycosylation profiling of human blood in type 2 diabetes patients. The glycan profiles of serum did not differ significantly between the heathy and patient samples, nevertheless, concentrations of two glycans in whole blood were found significantly higher in the case of patient samples suggesting possible new biomarkers of the disease.

Mátyás et al. [176] utilized the same separation matrix to compare *N*-glycan profiles of tomato xylem sap and found a statistical correlation between nutrient (nitrogen) deficiency symptoms on crops and changes in the glycan profile. Reider et al. [177] performed N-glycan profiling of PSA, which was isolated from urine using single domain antibodies immobilized on immobilized metal affinity chromatography columns. They were able to separate fucosylated and non-fucosylated structures as well as the α2,3- and α2,6-sialylated isomers, which is relevant to the cancer diagnosis as most common cancer-related alterations are associated with these structural changes.

The HR-NCHO separation gel buffer was further used for N-glycosylation characterization of omalizumab, an anti-asthma biotherapeutic mAb. The authors combined the CGE-LIF analysis with exoglycosidase array glycan sequencing. The exoglycosidases cleaved specific terminal monosaccharide units from glycan structures and this caused migration time shifts of their peaks, which was used to elucidate the structures [178]. Hurjak et al. [179] used the gel to analyze APTS-labeled N-glycans released from protective/inhibitory B subunits of human coagulation factor XIII.

Elucidation of glycan structures often requires large number of experiments and thus tends to be time-consuming. Multicapillary gel electrophoresis enables high-throughput analysis to overcome this problem. Filep et al. [180] used multi-capillary gel electrophoresis to analyze N-glycans from libraries containing carbohydrate structures most frequently occurring in biopharmaceuticals. They established a new glucose unit database to support large-scale N-glycosylation analysis in the biopharmaceutical sector. The viability of the library was demonstrated on the separation and identification of glycans released from adalimumab, a conventional therapeutic mAb, and etanercept, a new modality Fc-Fusion protein.

A high-throughput protocol using a CGE-LIF capillary array was proposed by Patenaude et al. [181] for total

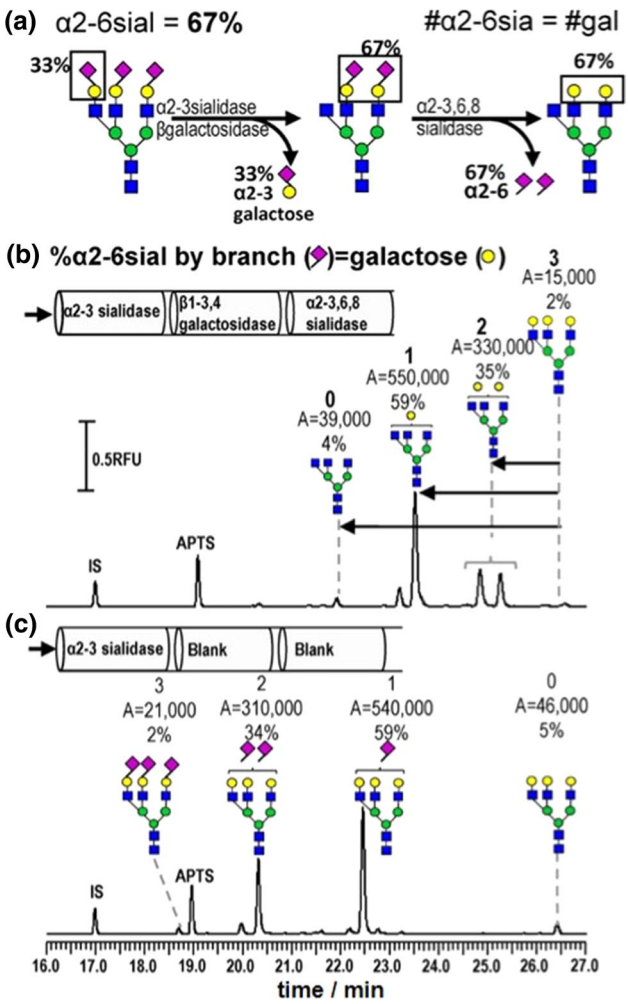

Fig. 5 Determination of α2,6-linked sialic acid with enzyme modification of glycans at the capillary inlet. **A** Reaction scheme showing that only galactoses linked to α2,6-linked sialic acids remain in the glycan after the enzyme treatment. **B** Electropherogram of an N-glycan standard with declared percentage of tri-antennary structures containing 0, 1, 2, and 3 α2,6-linked sialic acids of 4, 51, 36, and 5%, respectively. **C** Electropherogram from validation experiment with only one enzyme plug (α2-3-sialidase). Reprinted and edited with permission from Ref. [171]. Copyright 2020 American Chemical Society

N-glycan analysis of IgG isolated from mouse dried blood spots. Mice are recognized as a good experimental model for human IgG glycosylation. However, small blood volumes available from mice pose a challenge to glycomic studies. Extraction of glycans from dried blood spots improves the work with very low sample amounts.

Although gel matrix enhances the separation power and CGE-LIF is thus frequently used in glycomic analysis, capillary zone electrophoresis (CZE-LIF) separations in free solution prove to be a valuable tool as well. Huang et al. [182] used CZE-LIF to analyze cell surface N-glycans because cell surface proteins are important in drug target

screening and biomarker discovery. They captured the surface glycoproteins from intact Chinese hamster ovary cells on hydrazine-modified magnetic beads. Then N-glycans were released using PNGase F enzyme and labeled with APTS. Separation was performed in a commercial N-CHO-coated capillary using ammonium acetate buffer, pH 4.75 as a BGE.

Gel-free separation environment is often utilized in CE-MS because gel-containing BGEs are not compatible with ESI and MS. Szarka et al. [183] analyzed APTS-labeled linear malto-oligosaccharides and glycans released from human IgG 1 using ammonium acetate, pH 4.5 with 20% isopropanol as a BGE in a bare silica capillary. They used imaging LIF at the Taylor cone of ESI ion source. They simultaneously collected the data from fluorescence imaging and MS. MS data were used for qualitative analysis and fluorescence data for quantitation. Correlation of MS signal with LIF data helped to avoid possible misinterpretation of MS data caused by ion suppression, variations in ionization efficiency, unpredictable analyte fragmentation and rearrangement. On the other hand, mass spectra revealed several comigrating glycans that would not be distinguished using sole CE-LIF analysis.

In CE–MS, labeling of glycans is not always necessary. Váradi et al. [184] presented a CE–MS/MS method for label-free analysis of N-glycosylation combined with exoglycosidase sequencing to study alterations connected with Parkinson's disease. They developed a dynamic coating procedure for neutral capillary coating using polyethylene oxide to avoid the usage of polyvinyl alcohol coated capillaries that are incompatible with MS detection. BGE consisted of ammonium acetate, pH 5.0. They reported the most significantly altered levels of sialylation and fucosylation on tri- and tetra-antennary glycans of Parkinson's disease patients.

The same research group examined glycosylation of Cetuximab mAb drug using multiple fractionation and digestion strategies in combination with CE–MS profiling and LC–MS peptide mapping. Glycans were released by PNGase F in heavy water to allow the identification of potential glycosylation sites and site occupancy. N-Glycan structures were annotated using multiple exoglycosidase digestion steps in combination with CE-MS profiling. CE separations were performed in ammonium acetate buffer, pH 5.0. Site specificity was identified using C_4 reversed-phase fractionation. The glycosylation pattern was also examined across Cetuximab charge variant isoforms using cation-exchange chromatography with linear pH gradient elution followed by CE–MS profiling. Less common 2-AA glycan labeling was used in this study [185].

For in-depth studies of complex glycan samples, combination of mass detection with CE and LC can be highly advantageous. Song et al. [186] aimed at N-glycan characterization of urine exosomal components, including sulfated species, in healthy individuals to serve as a base for a non-invasive investigation into pathophysiological states of urinary system. They used CE-MS, MALDI-MS, and LC–MS/MS to identify N-glycan and sulfated N-glycan compositions. To resolve positional isomers of sialic acid, they utilized ion-exchange chromatography, microfluidic CE-LIF and MALDI-MS. They assigned the structures of the sialyl-linkage isomers through α2-3-sialidase treatment and sialic acid linkage-specific alkylamidation. They identified 219 N-glycans, including 175 compositions, 64 sialic acid linkage isomers, 26 structural isomers and 27 sulfated glycans. For CE-MS analysis, glycans were labeled with Girard's reagent T to incorporate a quaternary ammonium salt into their structure and thus enable their cathodic migration. They used a commercial coated capillary with neutral surface and 10% acetic acid as a BGE. For microfluidic CE-LIF, N-glycans were labeled with APTS. The authors fabricated a glass microfluidic chip with a cross-intersection for modified pinched injection and a 23 cm long serpentine separation channel. The channels were coated with poly(acrylamide) to provide neutral coating minimizing sample adsorption and EOF. They used HEPES buffer as a BGE.

A new CE-MS platform for in-depth glycome analysis of complex samples was introduced by Lageveen-Kammeijer [187]. For CE separation, they coated the capillary with Ultratrol dynamic coating. 10% acetic acid served as a BGE. They analyzed N-glycans released from total human plasma and identified 167 N-glycan compositions, including different sialic acid linkage variants. To deal with the complexity of the samples, they used linkage-specific derivatization of sialic acids. Ethyl esterification of α2,6-linked sialic acids (derivatized sialic acid mass was 319.127 Da) and amidation of α2,3-linked sialic acids (derivatized sialic acid mass was 290.111 Da) in a two-step one-pot reaction. This helped to overcome the instability of commonly used lacton-based derivatives. Reducing ends of N-glycans were derivatized with Girard's reagent P, carrying a permanent positive charge. As the sialic acid derivatization neutralized all N-glycans, they gained uniform charge enabling efficient ionization in positive mode.

An innovative approach was used by Jooß's research group [188]. They online coupled CZE with drift tube ion mobility mass spectrometry. They analyzed APTS-labeled N-glycans from A1GP and fetuin. The combination of mobility-based separation in liquid and gas phase brought dramatic increase in number of peaks observed. Each glycan resolved in CZE exhibited multiple peaks in ion mobility. They showed that each technique separately provided significantly lower performance than their combination. CZE separation was performed in a bare silica capillary with ε-aminocaproic acid/ammonia buffer in 50% methanol.

Glycans are not present only in glycoproteins. Glycosphingolipids are another example of biomolecules in which oligosaccharide chains play an important role. Glycosphingolipids are highly diverse surface-exposed biomolecules. Rossdam et al. [189] searched for cell surface markers to be used in the isolation of pure stem cell-derived cardiomyocytes (used as tissue transplants in regenerative medicine) from residual stem cells. They developed a high-throughput workflow for glycosphingolipid glycosylation profiling using APTS labeling of glycans and multiplexed GCE-LIF.

The same group studied also differential expression of glycosphingolipids in healthy and inflammatory conditions on a mouse model. They proposed that glycosphingolipids could serve as biomarkers for mapping genetic and homeostatic perturbances [190].

Conclusion

Glycans and glycopeptides are important biomolecules that are used, among others, as diseases biomarkers (breast cancer, hepatocellular carcinoma, Alzheimer's disease) and for monitoring their progression (qualitative and quantitative changes in glycosylation of proteins). Characterization of glycans and glycopeptides is crucial for the development of new biomarkers, glycoprotein-based drugs and for the evaluation of treatments. MS has been a powerful tool utilized for glycomic and glycoproteomic analysis due to its high sensitivity, speed, resolution, and rich structural information using different fragmentation techniques. However, separation step before MS, including mainly liquid chromatography and capillary electrophoresis, provides more confident identification and reliable quantitation of glycans and glycopeptides. Although LC–MS is the most used separation technique in glycoproteomic analysis, it is more expensive and time-consuming than CE methods. CE provides usually shorter analysis, is environment friendly, and has high separation efficiency. On the other hand, derivatization and/or labeling is necessary for CE methods in glycoproteomics. Moreover, CE–MS techniques require special MS interfaces and have high demand on experienced operators. Thus, LC–MS is more convenient for routine use in glycoproteomics than CE–MS.

The future target in glycoproteomics will be most likely focused on the structural analysis of glycans associated with specific sites which could help in clarifying of many biological and biochemical questions. Even though separation techniques undoubtedly help in structure elucidation of glycans and glycopeptides, mass spectrometry is still the key technique in glycoproteomics. Technology improvements of mass spectrometric instruments, e.g., hybrid-type fragmentation, orbitrap-based analyzer, ion mobility, connected with advanced search engines and algorithms incorporated in glycoproteomic software will play crucial role in comprehensive characterization of protein glycosylation.

This review summarizes the scientific literature related to liquid chromatography and capillary electrophoresis in glycomic and glycoproteomic analyzes. We have discussed advances in LC and CE techniques in the analysis of released glycans and intact glycopeptides. Understanding glycan and glycopeptide separations in LC and CE is crucial for the development of reliable and robust methods enabling comprehensive glycoproteome characterization.

Acknowledgements The authors are grateful for the financial support provided by the grant of Czech Science Foundation (No 19-18005Y) and by the Grant Agency of Charles University (No 336421). This review was supported in part by the Charles University project SVV260560 and Central European Exchange Program for University Studies, network RO-0010-16-2122—Teaching and Learning Bioanalysis.

References

1. Rudd P, Karlsson NG, Khoo KH, Packer NH (2017) Glycomics and Glycoproteomics. Cold Spring Harbor Laboratory Press, New York
2. An HJ, Froehlich JW, Lebrilla CB (2009) Curr Opin Chem Biol 13:421
3. Ohtsubo K, Marth JD (2006) Cell 126:855
4. Taylor ME, Drickamer K (2011) Introduction to Glycobiology. Oxford University Press, New York
5. Lowenthal MS, Davis KS, Formolo T, Kilpatrick LE, Phinney KW (2016) J Proteome Res 15:2087
6. Miyamoto S, Stroble CD, Taylor S, Hong Q, Lebrilla CB, Leiserowitz GS, Kim K, Ruhaak LR (2018) J Proteome Res 17:222
7. Scott DA, Drake RR (2019) Expert Rev Proteomics 16:665
8. Scott E, Munkley J (2019) Int J Mol Sci 20:1389
9. Ressom HW, Varghese RS, Goldman L, An Y, Loffredo CA, Abdel-Hamid M, Kyselova Z, Merchref Y, Novotny M, Drake SK, Goldman R (2008) J Proteome Res 7:603
10. Ng BG, Freeze HH (2018) Trends Genet 34:466
11. Haukedal H, Freude KK (2021) Front Neurosci 14:625348
12. Costa AR, Rodrigues ME, Henriques M, Oliveira R, Azeredo J (2014) Crit Rev Biotechnol 34:281
13. Jez J, Antes B, Castilho A, Kainer M, Wiederkum S, Grass J, Rüker F, Woisetschläger M, Steinkellner H (2012) J Biol Chem 287:24313
14. Zeng D, Debabov D, Hartsell TL, Cano RJ, Adams S, Schuyler JA, McMillan R, Pace JL (2016) Cold Spring Harb Perspect Med 6:a026989
15. Gong B, Burnina I, Stadheim TA, Li H (2013) J Mass Spectrom 48:1308
16. Qing G, Yan J, He X, Li X, Liang X (2020) Trends Anal Chem 124:115570
17. Ikegami T (2018) J Sep Sci 42:130
18. Peng W, Gutierrez-Reyes CD, Gautam S, Yu A, Cho BG, Goli M, Donohoo K, Mondello S, Kobeissy F, Mechref Y (2021). Mass Spectrom Rev. https://doi.org/10.1002/mas.21713

19. Gutierrez-Reyes CD, Jiang P, Donohoo K, Atashi M, Mechref Y (2020) J Sep Sci 44:403
20. Yin H, Zhu J (2022). Mass Spectrom Rev. https://doi.org/10.1002/mas.21771
21. Kozlik P, Goldman R, Sanda M (2018) Anal Bioanal Chem 410:5001
22. Tao S, Huang Y, Boyes BE, Orlando R (2014) Anal Chem 86:10584
23. Molnarova K, Kozlík P (2020) Molecules 25:4655
24. Huang Y, Nie Y, Boyes B, Orlando R (2016) J Biomol Tech 27:98
25. Van der Burgt YEM, Siliakus KM, Cobbaert CM, Ruhaak LR (2020) J Proteome Res 19:2708
26. Hinneburg H, Stavenhagen K, Schweiger-Hufnagel U, Pengelley S, Jabs W, Seeberger PH, Silva DV, Wuhrer M, Kolarich D (2015) J Am Soc Mass Spectrom 27:507
27. Cao L, Tolic N, Qu Y, Meng D, Zhao R, Zhang Q (2014) Anal Biochem 452:96
28. Alley WR, Mechref Y, Novotny MV (2009) Rapid Commun Mass Spectrom 23:161
29. Vekey K, Ozohanics O, Toth E, Jeko A, Revesz A, Krenyacz J (2013) Int J Mass Spectrom 345:71
30. Shao MC, Chin CCQ (1992) Anal Biochem 207:100
31. Zong G, Li C, Wang LX (2020) Methods Mol Biol 2103:249
32. Milla P, Ferrari F, Muntoni E, Sartori M, Ronco C, Arpicco S (2020) J Chromatogr B 1148:122151
33. Takegawa Y, Deguchi K, Ito H, Keira T, Nakagawa H, Nishimura SI (2006) J Sep Sci 29:2533
34. Takegawa Y, Deguchi K, Keira T, Ito H, Nakagawa H, Nishimura SI (2006) J Chromatogr A 1113:177
35. Benicky J, Sanda M, Pompach P, Wu J, Goldman R (2014) Anal Chem 86:10716
36. Darebna P, Novak P, Kucera R, Topolcan O, Sanda M, Goldman R, Pompach P (2017) J Proteomics 153:44
37. Medzihradszky KF, Besman MJ, Burlingame AL (1997) Anal Chem 69:3986
38. Yin H, An M, So P, Wong MYM, Lubman DM, Yao Z (2018) Electrophoresis 39:2351
39. Song E, Pyreddy S, Mechref Y (2012) Rapid Commun Mass Spectrom 26:1941
40. Gnanesh Kumar BS, Rawal A (2020) Int J Biol Macromol 155:605
41. Jinesh P, Lijina P, Gnanesh Kumar BS (2021) Amino Acids 53:533
42. Kozlik P, Goldman R, Sanda M (2017) Electrophoresis 38:2193
43. Molnarova K, Duris A, Jecmen T, Kozlik P (2021) Anal Bioanal Chem 413:4321
44. Tarasova IA, Masselon CD, Gorshkov AV, Gorshkov MV (2016) Analyst 141:4816
45. Badgett MJ, Boyes B, Orlando R (2017) J Biomol Tech 28:122
46. Ang E, Neustaeter H, Spicer V, Perreault H, Krokhin O (2019) Anal Chem 91:13360
47. Gilar M, Yu YQ, Ahn J, Xie H, Han H, Ying W, Qian X (2011) Anal Biochem 417:80
48. Kozlik P, Sanda M, Goldman R (2017) J Chromatogr A 1519:152
49. Hernandez-Hernandez O, Quintanilla-Lopez JE, Lebron-Aguilar R, Sanz ML, Moreno FJ (2016) J Chromatogr A 1428:202
50. Hong Q, Lebrilla CB, Miyamoto S, Ruhaak LR (2013) Anal Chem 85:8585
51. Sanda M, Zhang L, Edwards NJ, Goldman R (2016) Anal Bioanal Chem 409:619
52. Wang B, Tsybovsky Y, Palczewski K, Chance MR (2014) J Am Soc Mass Spectrom 25:729
53. Ozohanics O, Turiák L, Puerta A, Vékey K, Drahos L (2012) J Chromatogr A 1259:200
54. Camperi J, Combes A, Guibourdenche J, Guillarme D, Pichon V, Fournier T, Delaunay N (2018) J Pharm Biomed Anal 161:35
55. Ji ES, Lee HK, Park GW, Kim KH, Kim JY, Yoo JS (2019) J Chromatogr B 1110:101
56. Zhong J, Huang Y, Mechref Y (2021) Anal Chem 93:5763
57. Antonopoulos A, Broome S, Sharov V, Ziegenfuss C, Easton RL, Panico M, Dell A, Morris HR, Haslam SM (2020) Glycobiology 31:181
58. Gong Y, Qin S, Dai L, Tian Z (2021) Signal Transduct Target Ther 6:396
59. Zhou D, Tian X, Qi R, Peng C, Zhang W (2020) Glycobiology 31:69
60. Shajahan A, Supekar NT, Gleinich AS, Azadi P (2020) Glycobiology 30:981
61. Vankadari N, Wilce JA (2020) Emerg Microbes Infect 9:601
62. Sanda M, Morrison L, Goldman R (2021) Anal Chem 93:2003
63. Buszewski B, Noga S (2011) Anal Bioanal Chem 402:231
64. Veillon L, Huang Y, Peng W, Dong X, Cho BG, Mechref Y (2017) Electrophoresis 38:2100
65. Wuhrer M, de Boer AR, Deelder AM (2008) Mass Spectrom Rev 28:192
66. Hernandez-Hernandez O, Lebron-Aguilar R, Quintanilla-Lopez JE, Sanz ML, Moreno FJ (2010) Proteomics 10:3699
67. Furuki K, Toyo'oka T (2017) Biomed Chromatogr 31:e3988
68. Pedrali A, Tengattini S, Marrubini G, Bavaro T, Hemström P, Massolini G, Terreni M, Temporini C (2014) Molecules 19:9070
69. Tengattini S, Domínguez-Vega E, Temporini C, Bavaro T, Rinaldi F, Piubelli L, Pollegioni L, Massolini G, Somsen GW (2017) Anal Chim Acta 981:94
70. Bapiro TE, Richards FM, Jodrell DI (2016) Anal Chem 88:6190
71. Pereira L (2008) J Liq Chromatogr Relat Technol 31:1687
72. Forgács E (2002) J Chromatogr A 975:229
73. West C, Elfakir C, Lafosse M (2010) J Chromatogr A 1217:3201
74. Davies M, Smith KD, Harbin AM, Hounsell EF (1992) J Chromatogr A 609:125
75. Davies MJ, Smith KD, Carruthers RA, Chai W, Lawson AM, Hounsell EF (1993) J Chromatogr A 646:317
76. Fan JQ, Kondo A, Kato I, Lee YC (1994) Anal Biochem 219:224
77. Wagner-Rousset E, Bednarczyk A, Bussat MC, Colas O, Corvaïa N, Schaeffer C, Van Dorsselaer A, Beck A (2008) J Chromatogr B 872:23
78. Thaysen-Andersen M, Wilkinson BL, Payne RJ, Packer NH (2011) Electrophoresis 32:3536
79. Nwosu CC, Seipert RR, Strum JS, Hua SS, An HJ, Zivkovic AM, German BJ, Lebrilla CB (2011) J Proteome Res 10:2612
80. Alley WR, Mechref Y, Novotny MV (2009) Rapid Commun Mass Spectrom 23:495
81. Froehlich JW, Barboza M, Chu C, Lerno LA, Clowers BH, Zivkovic AM, German BJ, Lebrilla CB (2011) Anal Chem 83:5541
82. Hua S, Hu CY, Kim BJ, Totten SM, Oh MJ, Yun N, Nwosu CC, Yoo SJ, Lebrilla CB, An HJ (2013) J Proteome Res 12:4414
83. Donohoo KB, Wang J, Goli M, Yu A, Peng W, Hakim MA, Mechref Y (2022) Electrophoresis 43:119
84. Hua S, Nwosu CC, Strum JS, Seipert RR, An HJ, Zivkovic AM, German BJ, Lebrilla CB (2011) Anal Bioanal Chem 403:1291
85. Nwosu CC, Huang J, Aldredge DL, Strum JS, Hua S, Seipert RR, Lebrilla CB (2012) Anal Chem 85:956
86. Zhu R, Huang Y, Zhao J, Zhong J, Mechref Y (2020) Anal Chem 92:9556
87. Pirok BWJ, Gargano AFG, Schoenmakers PJ (2018) J Sep Sci 41:68
88. Dugo P, Cacciola F, Kumm T, Dugo G, Mondello L (2008) J Chromatogr A 1184:353
89. Iguiniz M, Heinisch S (2017) J Pharm Biomed 145:482
90. Stoll DR, Carr PW (2017) Anal Chem 89:519

91. Zhang X, Fang A, Riley CP, Wang M, Regnier FE, Buck C (2010) Anal Chim Acta 664:101
92. Lam MPY, Siu SO, Lau E, Mao X, Sun HZ, Chiu PCN, Yeung WSB, Cox DM, Chu IK (2010) Anal Bioanal Chem 398:791
93. Lam MPY, Lau E, Siu SO, Ng DCM, Kong RPW, Chiu PCN, Yeung WSB, Lo C, Chu IK (2011) Electrophoresis 32:2930
94. Lewandrowski U, Sickmann A (2010) Anal Chem 82:5391
95. Zhao Y, Szeto SSW, Kong RPW, Law CH, Li G, Quan Q, Zhang Z, Wang Y, Chu IK (2014) Anal Chem 86:12172
96. Stavenhagen K, Plomp R, Wuhrer M (2015) Anal Chem 87:11691
97. Merry T, Astrautsova S (2013) Capillary electrophoresis of carbohydrates. Humana Press, New Jersey
98. Tarentino AL, Gomez CM, Plummer TH (1985) Biochemistry 24:4665
99. Szigeti M, Bondar J, Gjerde D, Keresztessy Z, Szekrenyes A, Guttman A (2016) J Chromatogr B 1032:139
100. Vilaj M, Lauc G, Trbojević-Akmačić I (2020) Glycobiology 31:2
101. Huang Y, Orlando R (2017) J Biomol Tech 28:150
102. Jmeian Y, Hammad LA, Mechref Y (2012) Anal Chem 84:8790
103. Lingg N, Zhang P, Song Z, Bardor M (2012) Biotechnol J 7:1462
104. Jensen PH, Kolarich D, Packer NH (2009) FEBS J 277:81
105. Miura Y, Kato K, Takegawa Y, Kurogochi M, Furukawa J, Shinohara Y, Nagahori N, Amano M, Hinou H, Nishimura SI (2010) Anal Chem 82:10021
106. Furuki K, Toyo'oka T, Ban K (2017) Anal Bioanal Chem 409:2269
107. Wang C, Fan W, Zhang P, Wang Z, Huang L (2011) Proteomics 11:4229
108. Pompach P, Chandler KB, Lan R, Edwards N, Goldman R (2012) J Proteome Res 11:1728
109. Huang Y, Zhou S, Zhu J, Lubman DM, Mechref Y (2017) Electrophoresis 38:2160
110. Sriwilaijaroen N, Nakakita S, Kondo S, Yagi H, Kato K, Murata T, Hiramatsu H, Kawahara T, Watanabe Y, Kanai Y, Ono T, Hirabayashi J, Matsumoto K, Suzuki Y (2018) FEBS J 285:1611
111. Barbosa EA, Fontes NDC, Santos SCL, Lefeber DJ, Bloch C, Brum JM, Brand GD (2019) Clin Chim Acta 492:102
112. Bones J, Mittermayr S, O'Donoghue N, Guttman A, Rudd PM (2010) Anal Chem 82:10208
113. Zhou S, Veillon L, Dong X, Huang Y, Mechref Y (2017) Analyst 142:4446
114. Vreeker GCM, Wuhrer M (2017) Anal Bioanal Chem 409:359
115. Dong X, Zhou S, Mechref Y (2016) Electrophoresis 37:1532
116. Oursel S, Cholet S, Junot C, Fenaille F (2017) J Chromatogr B 1071:49
117. Porfirio S, Archer-Hartmann S, Moreau GB, Ramakrishnan G, Haque R, Kirkpatrick BD, Petri WA, Azadi P (2020) Glycobiology 30:774
118. Kurz S, Sheikh MO, Lu S, Wells L, Tiemeyer M (2021) Mol Cell Proteom 20:100045
119. Cho BG, Veillon L, Mechref Y (2019) J Proteome Res 18:3770
120. Gautam S, Peng W, Cho B, Huang Y, Banazadaeh A, Yu A, Dong X, Mechref Y (2020) Analyst 145:6656
121. Cho BG, Jiang P, Goli M, Gautam S, Mechref Y (2021) Analyst 146:4374
122. Palmigiano A, Messina A, Sturiale L, Garozzo D (2018) Advances in the Use of Liquid Chromatography Mass Spectrometry (LC-MS): Instrumentation Developments and Applications. Elsevier, Amsterdam
123. Suzuki N, Abe T, Natsuka S (2019) Anal Biochem 567:117
124. Jeong YR, Kim SY, Park YS, Lee GM (2018) J Pharm Sci 107:1831
125. Walker SH, Carlisle BC, Muddiman DC (2012) Anal Chem 84:8198
126. Walker SH, Lilley LM, Enamorado MF, Comins DL, Muddiman DC (2011) J Am Soc Mass Spectrom 22:1309
127. Ruhaak LR, Huhn C, Waterreus WJ, de Boer AR, Neusüss C, Hokke CH, Deelder AM, Wuhrer M (2008) Anal Chem 80:6119
128. Lauber MA, Yu YQ, Brousmiche DW, Hua Z, Koza SM, Magnelli P, Guthrie E, Taron CH, Fountain KJ (2015) Anal Chem 87:5401
129. Ahn J, Bones J, Yu YQ, Rudd PM, Gilar M (2010) J Chromatogr B 878:403
130. Zhang X, Reed CE, Birdsall RE, Yu YQ, Chen W (2020) SLAS Technol 25:380
131. Mauko L, Nordborg A, Hutchinson JP, Lacher NA, Hilder EF, Haddad PR (2011) Anal Biochem 408:235
132. Tousi F, Bones J, Hancock WS, Hincapie M (2013) Anal Chem 85:8421
133. Adamczyk B, Tharmalingam-Jaikaran T, Schomberg M, Szekrényes Á, Kelly RM, Karlsson NG, Guttman A, Rudd PM (2014) Carbohydr Res 389:174
134. Kawasaki N, Ohta M, Hyuga S, Hashimoto O, Hayakawa T (1999) Anal Biochem 269:297
135. Hua S, An HJ, Ozcan S, Ro GS, Soares S, DeVere-White R, Lebrilla CB (2011) Analyst 136:3663
136. Mauko L, Lacher NA, Pelzing M, Nordborg A, Haddad PR, Hilder EF (2012) J Chromatogr B 911:93
137. Pabst M, Bondili JS, Stadlmann J, Mach L, Altmann F (2007) Anal Chem 79:5051
138. Stadlmann J, Pabst M, Kolarich D, Kunert R, Altmann F (2008) Proteomics 8:2858
139. Karlsson NG, Wilson NL, Wirth HJ, Dawes P, Joshi H, Packer NH (2004) Rapid Commun Mass Spectrom 18:2282
140. She YM, Tam RY, Li X, Rosu-Myles M, Sauvé S (2020) Anal Chem 92:14038
141. Zhou S, Huang Y, Dong X, Peng W, Veillon L, Kitagawa DAS, Aquino AJA, Mechref Y (2017) Anal Chem 89:6590
142. Jin C, Harvey DJ, Struwe WB, Karlsson NG (2019) Anal Chem 91:10604
143. Bäckström M, Thomsson KA, Karlsson H, Hansson GC (2009) J Proteome Res 8:538
144. Deguchi K, Keira T, Yamada K, Ito H, Takegawa Y, Nakagawa H, Nishimura SI (2008) J Chromatogr A 1189:169
145. Cao C, Yu L, Yan J, Fu D, Yuan J, Liang X (2021) Talanta 221:121382
146. Stoll DR, Harmes DC, Staples GO, Potter OG, Dammann CT, Guillarme D, Beck A (2018) Anal Chem 90:5923
147. Štěpánová S, Kašička V (2022) Anal Chim Acta 1209:339447
148. Camperi J, Pichon V, Delaunay N (2020) J Pharm Biomed 178:112921
149. Puerta A, Gomez-Ruiz L, Diez-Masa JC, de Frutos M (2021) Carbohydrate analysis by modern liquid phase separation techniques. Elsevier, Amsterdam
150. Amon S, Zamfir AD, Rizzi A (2008) Electrophoresis 29:2485
151. Sanz-Nebot V, Balaguer E, Benavente F, Neusüss Ch, Barbosa J (2007) Electrophoresis 28:1949
152. Haselberg R, de Jong GJ, Somsen GW (2013) Anal Chem 85:2289
153. Haselberg R, De Vijlder T, Heukers R, Smit MJ, Romijn EP, Somsen GW, Domínguez-Vega E (2018) Anal Chim Acta 1044:181
154. Ongay S, Neusüss CH (2010) Anal Bioanal Chem 398:1618
155. Kammeijer GSM, Jansen B, Kohler I, Heemskerk AAM, Mayboroda OA, Hensbergen PJ, Schappler J, Wuhrer M (2017) Sci Rep 7:3733
156. Fuguet E, Ràfols C, Bosch E, Rosés M (2009) Chem Biodivers 6:1822

157. Kammeijer GSM, Nouta J, de la Rosette JJMCH, de Reijke TM, Wuhrer M (2018) Anal Chem 90:4414
158. Amon S, Plematl A, Rizzi A (2006) Electrophoresis 27:1209
159. Zhang Ch, Bi C, Clarke W, Hage DS (2017) J Chromatogr A 1523:114
160. Lu G, Crihfield CL, Gattu S, Veltri LM, Holland LA (2018) Chem Rev 118:7867
161. Fomin MA, Seikowski J, Belov VN, Hell SW (2020) Anal Chem 92:5329
162. Khan S, Liu J, Szabo Z, Kunnummal B, Han X, Ouyang Y, Linhardt RJ, Xia Q (2018) Rapid Commun Mass Spectrom 32:882
163. Krenkova J, Dusa F, Cmelik R (2020) Electrophoresis 41:684
164. Krenkova J, Liskova M, Cmelik R, Vigh G, Foret F (2020) Anal Chim Acta 1095:226
165. Kinoshita M, Yamada K (2022) J Pharm Biomed Anal 207:114424
166. Liénard-Mayor T, Yang B, Tran NT, Bruneel A, Guttman A, Taverna M, Mai TD (2021) J Chromatogr A 1657:462593
167. Shao H, Reider B, Jarvas G, Guttman A, Jiang Z, Tran NT, Taverna M (2020) Anal Chim Acta 1134:1
168. Gattu S, Crihfield CL, Holland LA (2017) Anal Chem 89:929
169. Wu X, Langan TJ, Durney BC, Holland LA (2017) Electrophoresis 33:2676
170. Lu G, Holland LA (2019) Anal Chem 91:1375
171. Bwanali L, Crihfield CL, Newton EO, Zeger VR, Gattu S, Holland LA (2020) Anal Chem 92:1518
172. Giron LB, Papasavvas E, Azzoni L, Yin X, Anzurez A, Damra M, Mounzer K, Kostman JR, Sanne I, Firnhaber CS, Tateno H, Liu Q, Montaner LJ, Abdel-Mohsen M (2020) AIDS 34:681
173. Mészáros B, Járvás G, Farkas A, Szigeti M, Kovács Z, Kun R, Szabó M, Csánky E, Guttman A (2020) J Chromatogr B 1137:121913
174. Mészáros B, Járvás G, Kun R, Szabó M, Csánky E, Abonyi J, Guttman A (2020) Cancers 12:3700
175. Torok R, Horompoly K, Szigeti M, Guttman A, Vitai M, Koranyi L, Jarvas G (2021) Molecules 26:6399
176. Mátyás B, Singer J, Szarka M, Lowy DA, Döncző B, Makleit P, Failoc-Rojas VE, Ramirez A, Martínez P, Sándor Z, Kincses I, Guttman A (2021) Electrophoresis 42:200
177. Reider B, Gacsi E, Jankovics H, Vonderviszt F, Szarvas T, Guttman A, Jarvas G (2021) Anal Chim Acta 1184:338892
178. Szabo M, Filep C, Nagy M, Sarkozy D, Szigeti M, Sperling E, Csanky E, Guttman A (2022) J Pharm Biomed Anal 209:114483
179. Hurják B, Kovács Z, Döncző B, Katona É, Haramura G, Erdélyi F, Housang Shemirani A, Sadeghi F, Muszbek L, Guttman A (2020) J Thromb Haemost 18:1302
180. Filep C, Borza B, Jarvas G, Guttman A (2020) J Pharm Biomed Anal 178:112892
181. Patenaude AM, Erhardt J, Hennig R, Rapp E, Lauc G, Pezer M (2021) Electrophoresis 42:2615
182. Huang J, Bian X, Chang K, Hou L, Feng H (2019) Chromatographia 82:1079
183. Szarka M, Szigeti M, Guttman A (2019) Anal Chem 91:7738
184. Váradi C, Nehéz K, Hornyák O, Viskolcz B, Bones J (2019) Molecules 24:2220
185. Váradi C, Jakes C, Bones J (2020) J Pharm Biomed Anal 180:113035
186. Song W, Zhou X, Benktander JD, Gaunitz S, Zou G, Wang Z, Novotny MV, Jacobson SC (2019) Anal Chem 91:13528
187. Lageveen-Kammeijer GSM, de Haan N, Mohaupt P, Wagt S, Filius M, Nouta J, Falck D, Wuhrer M (2019) Nat Commun 10:2137
188. Jooß K, Meckelmann SW, Klein J, Schmitz OJ, Neusüß C (2019) Anal Bioanal Chem 411:6255
189. Rossdam C, Konze SA, Oberbeck A, Rapp E, Gerardy-Schahn R, von Itzstein M, Buettner FFR (2019) Anal Chem 91:6413
190. Jirmo AC, Rossdam C, Grychtol R, Happle C, Gerardy-Schahn R, Buettner FFR, Hansen G (2020) Immun Inflamm Dis 8:512